3-Aminocoumarin based mononuclear complexes [M(1,1-dithiolato)$_n$] {Mn(II), Co(III), Zn(II) and Cd(II)}: Spectral characterization, fluorescence, optical and thermogravimetric study

Abstract

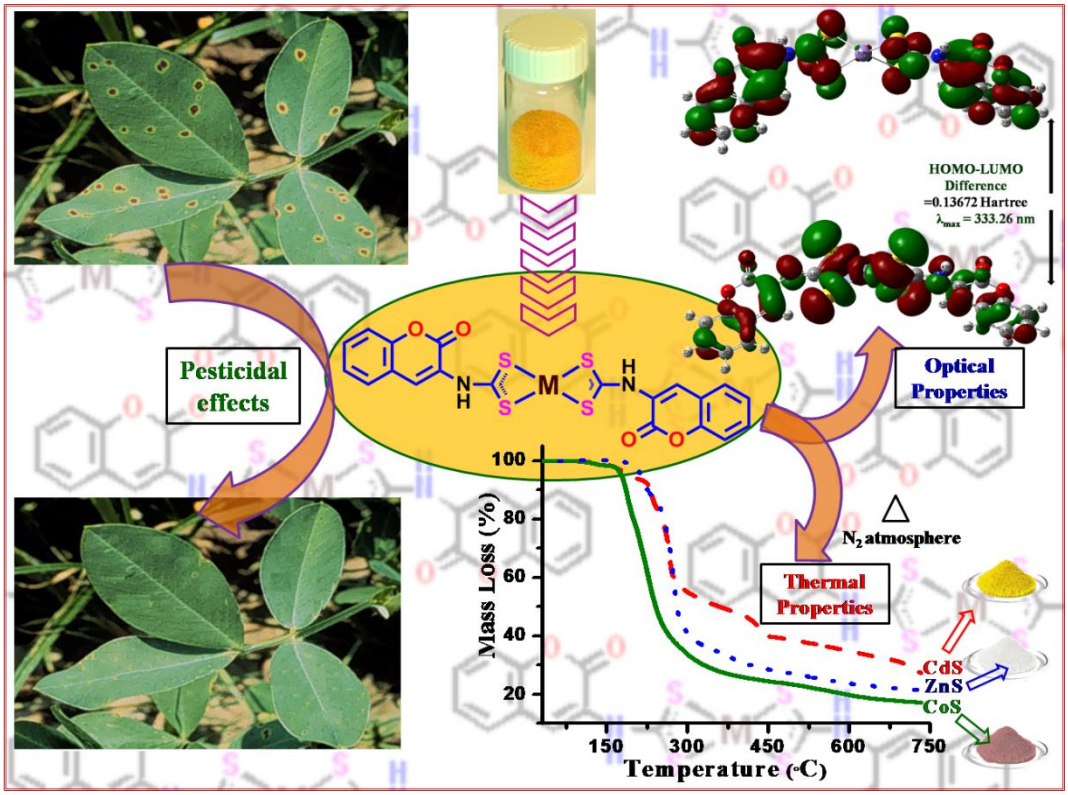

A series of neutral monometallic complexes [M(1,1-dithiolato)$_n$] {1,1-dithiolato = 3-dithiocarbamato coumarin; M = Mn(II), **1**; Co(III) **2**, Zn(II) **3** and Cd(II) **4**; n = 2 for **1**, **3, 4** and n = 3 for complex **2**}, was efficiently synthesized in a single pot reaction using 3-amino coumarin, CS_2 and $M(OAc)_2$. All the complexes were characterized by microanalysis, ESI MS, FT-IR, ^1H and ^{13}C NMR, UV-visible absorption, fluorescence, magnetic susceptibility and thermogravimetric studies. Evidently the 3-dithiocarbamato coumarin ligand behaves as a monobasic bidentate in all the complexes. The electronic absorption and magnetic moment data support a tetrahedral/ distorted tetrahedral geometry around Mn(II), Zn(II), Cd(II) and octahedral geometry around Co(III) centres. The fluorescence spectra of all complexes exhibit concomitant bathochromic shifts of the intra-molecular (CT→M) charge-transfer emissions. Interestingly, the thermal decomposition of the complexes

2-3 gave metal sulphide as a final product and indicates that these complexes may provide a single source material for the preparation of metal sulphide nanoparticles. The calculated band gap energies (Eg) fall in the range of 2.039-2.565 eV, suggesting a feature of direct band gap semiconducting nature for these complexes **1–4**.

3A.1. Introduction

The interest in the chemistry of metal complexes containing sulphur rich ligands has been continued because of their wide applications in the area of electrical conductivity, molecular magnetism, electrochemical, biological processes and optoelectronic properties [1]. Particularly, polydentate dithiocarbamate ligands have emerged as one of the most active parts of research in chemistry due to their versatile coordination chemistry, material properties and industrial applications [2]. They are ideal candidates to use extensively in the separation techniques [3] due to their ability to form stable chelates with a number of metal ions. They are also been used in the medicine due to the existence of dithiocarbamate moiety in a variety of biologically active molecules [4].

Apart from this, dithiocarbamate complexes with direct metal–sulfur bond as a single source precursor, has proven to be a very efficient and an alternative route for the synthesis of high-quality semi-conductor nanoparticles [5]. It appears that many of these complexes are used for the production of lead, cadmium, zinc, mercury and copper sulphides [6].

Thermogravimetric study of metal dithiocarbamate complexes suggests their wide spread industrial applications such as foam rubber, fungicides, effective heat stabilizers, antioxidant action, reprocessing of polymers etc [7]. It further suggests the suitability of complexes to be used as single source precursors for the synthesis of metal sulphide nano particles and thin films [8]. It has been found that the size and shape of the metal sulphide nanoparticles greatly depend on the nature of organic moiety present in metal dithiocarbamate complexes [9] which consecutively affect the fundamental properties such as optical, electrical and mechanical [10].

Although a wide range of biological activities, including CNS depressant, antibacterial, antiallergic and insect-growth regulatory effects have been shown by the derivatives of 3-amino coumarin [11] and antimicrobial, antioxidant activities by their transition metal complexes, [12] no attempt has been made so far to investigate the

synthesis, stability, structure and reactivity of dithiocarbamate derivative of 3-amino coumarin. In the present work we have demonstrated the one pot synthesis of a novel series of [M(1,1-dithiolato)$_n$] {1,1-dithiolato = 3-dithiocarbamato coumarin; M = Mn(II), **1**; Co(III) **2**, Zn(II) **3** and Cd(II) **4**; n = 2 for **1**, **3, 4** and n = 3 for complex **2**} complexes. These complexes are thoroughly characterized by Microanalysis, ESI MS, FT-IR, ^{1}H and ^{13}C NMR, UV-visible absorption, magnetic susceptibility and thermogravimetric studies. The fluorescence, optical and thermal behaviours were investigated.

3A.2. Results and Discussion

3A.2.1. Synthesis and characterization

One pot three component reaction of 3-amino coumarin, CS_2 and corresponding metal acetates in a basic solvent Et_3N at room temperature has yielded a novel series of coumarin based monometallic complexes [M(3-dithiocarbamato coumarin)$_n$] (**1–4**) as shown in Scheme 1. Carrying out several chemical operations simultaneously in a single vessel referred as the one-pot or domino or tandem reactions. This type of reaction has several distinctive advantages such as it can reduce the purifications of the intermediate compounds, predominantly important with unstable intermediates and may eventually save valuable resources.

The 2-pyrone (lactone) ring of the coumarin system is partially aromatic [13], and 3-amino coumarins as such behave like enamines and known to undergo hydrolysis under acidic conditions [14]. Thus the use of basic solvent, not only helped to protect 3-amino cumarin from hydrolysis but also helps in scavenging the -NH proton and thereby stabilizing *in situ* the dithiocarbamate –NCS_2 ligand moiety. It may be noted that under similar reaction condition, corresponding copper(II) and Ni(II) complex could not be obtained, instead diethyldithiocarbamate complex of copper(II) [15] and Ni(II) [16] were formed even when the reaction was performed using HPLC grade Et_3N. It appears that Et_2NH required for the formation of thermodynamically more stable diethyldithiocarbamate complexes is being formed during the reaction by the decomposition of Et_3N. The structures of all new complexes **1-4** were verified by microanalyses, thermal analysis, relevant spectroscopic methods, and confirmed by mass analysis. Further, the structure of Mn(II) complex **1** is optimized by performing DFT level optimization.

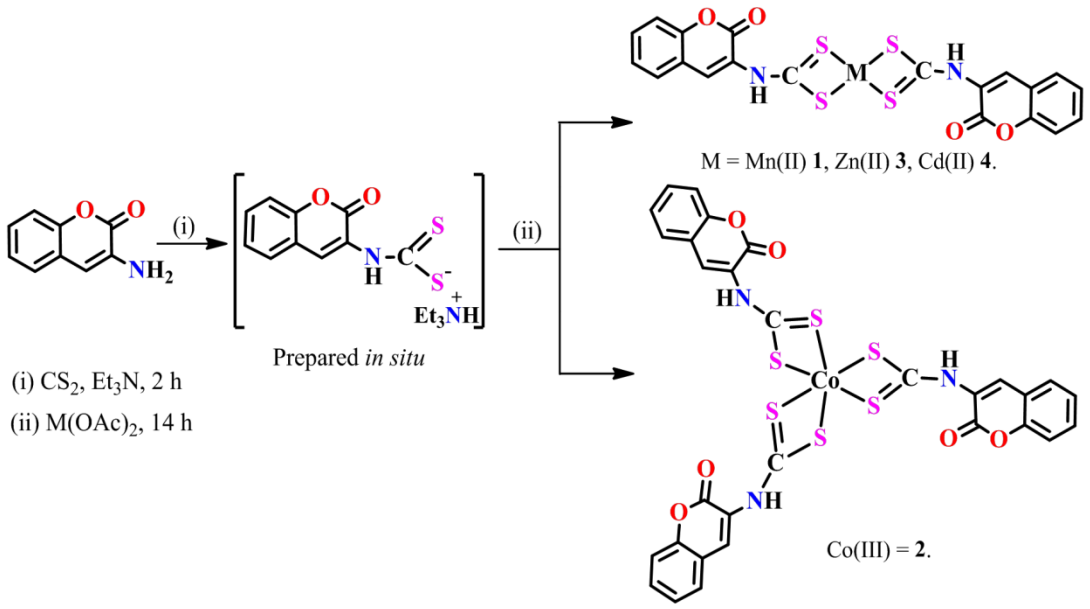

Scheme 1: Synthesis of metal complexes **1-4**.

The mechanism for the formation of triethyl ammonium salt of 3-dithiocarbamato coumarin can be illustrated as follows:

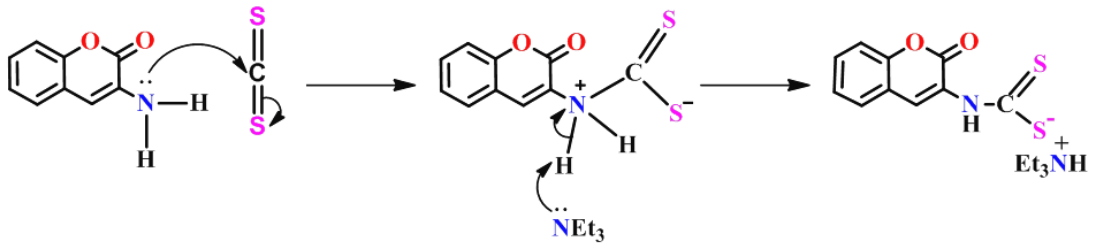

3A.2.2. IR Spectral study

The IR spectra of all complexes **1-4** were analyzed on the basis of general references [17] and further compared with other related compounds [18]. The characteristic IR bands of the complexes **1-4** are summarized in the experimental section. The disappearance of one of the υ(N-H) band corresponding to 3-amino coumarin (supporting information) in all the 3-dithiocarbamato coumarin complexes **1-4** and the appearance of new bands corresponding to υ(C–S) of dithiocarbamate moiety confirms the formation of complexes **1-4**. The mode of binding of dithiocarbamate ligand moiety can be clearly seen in the IR spectrum of the complexes. The presence of a single sharp medium intensity band at 933, 1015, 928 and 925 cm^{-1} in the IR spectrum of complexes 1, 2, 3 and 4 respectively, supports the

bidentate binding mode of 3-dithiocarbamato coumarin ligand. In addition to these new bands, all complexes exhibit bands in the range of 3330-3245, 3069-3040, 1728-1713, 1565-1511 and ~1180 cm^{-1} due to υ(N–H), υ(C–H), υ(C=O), υ(C–N)/(C=N), υ(C–O) stretching frequencies respectively which are associated with coumarin moiety in the complexes **1-4**. It is to be noted a peak observed at 1457 cm^{-1} attributed to the υ(C–N) in the 3-amino coumarin (supporting information) was shifted to higher frequency (1565–1511 cm^{-1}) in the complexes. This is due to the mesomeric drift of an electron cloud of the dithiocarbamate (–NCS_2) moiety towards the metal ion and confirmed an increase in the C–N double bond character. In the IR spectra of all the complexes, a sharp band in the range of 1728 cm^{-1} to 1713 cm^{-1} was observed. This has been assigned to the lactone ring carbonyl stretching frequency. The lack of any noticeable shift of the lactone ring carbonyl stretching frequencies as well as ring υ(C-O) frequencies in the complexes as compared with the corresponding band in the free 3-amino coumarin, confirms that the ring carbonyl and oxygen atom of coumarin ring did not participate in coordination with the metal ions in all these complexes [19]. Moreover the IR spectrum of complex **3** recorded in the far IR region exhibits the expected medium band 436 cm^{-1} assigned to the M–S stretching vibration indicating the gem-disulphur ligand [20].

From the IR data, it has been concluded that the 3-dithiocarabamato coumarin ligand behaves monobasic bidentate in the complexes **1-4**. Further it confirms the non-involvement of lactone ring carbonyl (>C=O) and ethereal C-O-C ring oxygen atoms in the bonding with the various metal centres.

3A.2.3. NMR spectral study

The diamagnetic complexes **2-4** were characterized by ^{1}H and ^{13}C NMR spectroscopy and the NMR data are summarized in the experimental section. In the ^{1}H NMR spectra of complexes **3** and **4**, the most characteristic signal observed at δ 9.078 ppm and δ 9.063 ppm are due to –NH proton respectively. The appearance of three –N*H* signals at 9.37, 9.12, 9.06 ppm in the ^{1}H spectrum and two –N*C*S_2 signals at 208.04, 203.27 ppm in the ^{13}C spectrum of complex **2**, suggest a different chemical environment of coordinated ligand moieties of complex **2** in solution. Beside this a significant downfield shifting of residual signals corresponding to the coumarin moiety of **2** in the ^{1}H and ^{13}C NMR spectra *ca* 7.62-7.31 ppm and 158.16-116.60 ppm

respectively, compared to free 3-amino coumarin, has been observed. A very downfiled shifting of to –NH proton as compared to its position δ 4.32 ppm observed in free 3-amino coumarin (supporting information) suggest the presence of dithiocarbamate moiety and responsible for strong deshielding –NH protons in these complexes. Apart from this, a significant downfiled shifting of aromatic signals of coumarin moiety of complexes **3** and **4** to δ 6.93-8.447 ppm and δ 6.93-8.436 ppm respectively as compared to the corresponding signals observed at 6.72-7.31ppm in free 3-amino coumarin, has been observed. Further the appearance of a very downfield signal at ~176 ppm in the ^{13}C NMR spectra of **3** and **4** which indeed a characteristic feature of coordinated dithiocarbamate moiety primarily derived from primary amine precursors [21], confirms the formation of 3-dithiocarbamato coumarin complexes **3** and **4**. Contrary to complex **3** and **4**, hefty downfield shifting of dithiocarbamate ($–NCS_2$) signals of complex **2** at 208.04, 203.27 ppm has been observed due to the coordination of dithiocarmate moieties to Co(III) centre. Moreover, the signals appeared at δ =163.93 and δ = 163.82 ppm, δ=157.23 and δ=157.24 ppm in the ^{13}C NMR spectra of **3** and **4** respectively are assignable to lactone ring carbonyl and conjugated C=N groups present in these complexes. The number of ^{1}H and ^{13}C NMR signals and their splitting patterns suggest that both 3-dithiocarbamato coumarin ligands are in different chemical environments in the complexes **3** and **4**.

3A.2.4. Electronic absorption spectral and magnetic moment study

The electronic absorption spectral data of 3-amino coumarin and new 3-dithiocarbamato metal complexes **1-4** in 10^{-5} M DMSO solution are given in Table 1 and tentative assignments of the important characteristic bands have been made with the help of an earlier publication [18, 22- 24].

Table 1. UV-visible and fluorescence and optical band gap data of complexes 1-4.

Entry	UV-Visible spectral data (10^{-5} M DMSO) λ_{max} nm (ε, L mol^{-1} cm^{-1})		Magnetic moment μ_{eff} (BM)	Fluorescence spectral data (10^{-5} M DMSO) λ_{em} nm		λ_{ex} (nm)	Band Gap Ea (eV)
3-amino-coumarin	259 (30984)	π→π*	--	422	π*→ π	259	--
	332 (94552)	n→π*					
1	259 (34683))	π→π*	6.78	409	π*→ π	259	2.547
	326 (83162)	n→π*		518			
	450 (3429)	charge transfer					

2	259 (62245)	π→π*	0.0	470	π*→ π	259	2.039
	337 (79498)	n→π*		518			
	416 (39070)	charge transfer					
	640 (1072)	$^1A_{1g}(F)\rightarrow{}^1B_{1g}$					
3	293 (62681)	π→π*	0.0	485	π*→π	293	2.565
	331 (55241)	n→π*					
	407 (69912)	charge transfer					
4	293 (50585)	π→π*	0.0	483	π*→ π	293	2.544
	334 (49363)	n→π*					
	404 (58131)	charge Transfer					

The magnetic moment data are also summarized in Table1 and the nature of the ligand field around the metal ion has been deduced from the electronic spectra (Fig. 1) and the magnetic moment values of the complexes. The electronic absorption spectrum of 3-amino coumarin gives two bands at 259 and 332 nm which are mainly attributed to the π – π* and n – π* transitions possibly occurring due to the lactone oxygen of the coumarin moiety [23]. The 3-amino coumarin and complexes **1-4**, exhibit maximum absorbance at 332, 326, 337, 407 and 404 nm with the molar extinction coefficient values of 94552, 83162, 79498, 69912 and 58131 respectively. A significant bathochromic shift (red shift of approx 34) of one of the bands observed at 259 in the free 3-amino coumarin was seen in the 3-dithiocarbamato complexes of Zn(II) **3** and Cd(II) **4**. The new bands appeared at 450, 416, 407 and 404 nm in the electronic absorption spectra of all the complexes **1-4**, are attributed to charge transfer processes, probably, from ligand to metal, mainly associated with dithiocarbamate (-NCS_2) moiety [22, 24]. Apart from this, complex **2** exhibits a weak *d-d* band at 640 nm, arises due to $^1A_{1g}(F)\rightarrow{}^1B_{1g}$ transition. The UV-visible bands together with microanalysis and NMR data suggests the octahedral geometry around the Co(III) centre [25] in complex **2.**

Moreover, the *d-d* bands of high-spin Mn(II) complexes have extremely low intensity and in the presence of organic ligands and they could rarely be detected [26]. Thus, based on IR and electronic spectral studies and calculated magnetic moment value of 6.78 BM, a distorted tetrahedral geometry around Mn(II) is proposed and latterly confirmed by DFT level optimization. The room temperature magnetic moment values and electronic spectral bands are consistent with a tetrahedral/distorted tetrahedral [27] coordination geometry around the Zn(II) and Cd(II) centres in complexes **3** and **4** respectively.

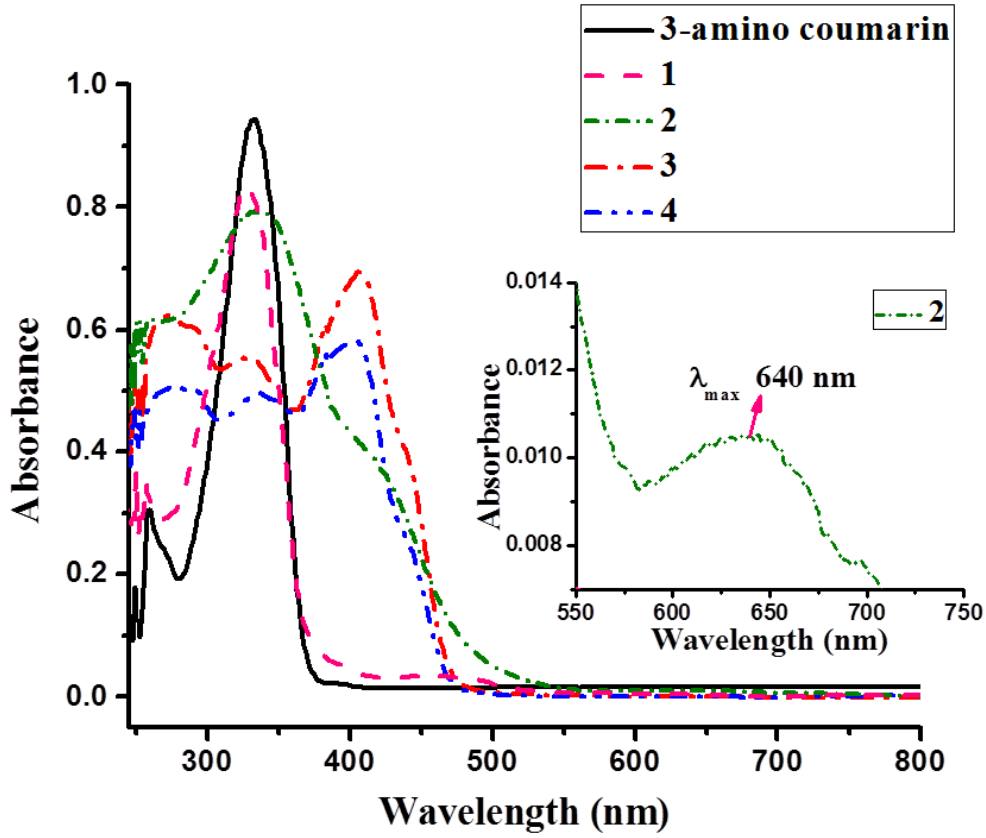

Fig. 1. UV-visible absorption spectra of the ligand precursor and bis-dithiocarbamate metal complexes at room temperature in 10^{-5} M DMSO solution.

3A.2.5. Fluorescence spectral study

The fluorescence properties of the ligand precursor 3-amino coumarin and the complexes **1-4** studied at room temperature (298 K) in the10^{-5}M DMSO solution and the spectral data is summarized in Table 1. The fluorescence spectra of these compounds are shown in Fig. 2. The ligand precursor 3-amino coumarin shows a fluorescence band at 422 nm upon excitation at either λ_{ex} = 259 nm or 332 nm. However complexes **1** and **2** upon excitation at λ_{ex} = 259 nm display a significant fluorescence emission band at 409 nm (Stokes shifts of ≈ 150 nm) and 468 nm (Stokes shifts of ≈ 209 nm) respectively along with a weak intensity band at 518 nm respectively due to excitation overtone. It may be noted that the complexes **1** and **2** upon excitation at λ_{ex} = 326 nm and 337 nm respectively showed emission bands similar to their respective emissions observed upon excitation at λ_{ex} = 259 nm. Furthermore these complexes **1** and **2** display emission bands at 535 nm and 477 nm

upon excitation at λ_{ex} = 450 nm and 416 nm respectively due to charge transfer de-excitation in pathways (supplementary information).

Evidently complexes **3** and **4** exhibit similar emission patterns upon excitation at different wavelengths. For instance an emission band at 485 nm is observed upon excitation of complex **3** at λ_{ex} = 293, 331 or 407 nm whereas an emission band at 483 nm is observed upon excitation of complex **4** at λ_{ex} = 293, 334 or 404 nm.

Such a trend of fluorescence spectra and concomitant bathochromic shifts of intramolecular charge-transfer emissions by coordination compounds were previously observed in dithiocarbamate [15], dialkoxo-bridged [28] and Salen-type [30] complexes. The fluorescence behaviour of these complexes may be attributed to the reduction of photoinduced electron transfer process on complex formation [30].

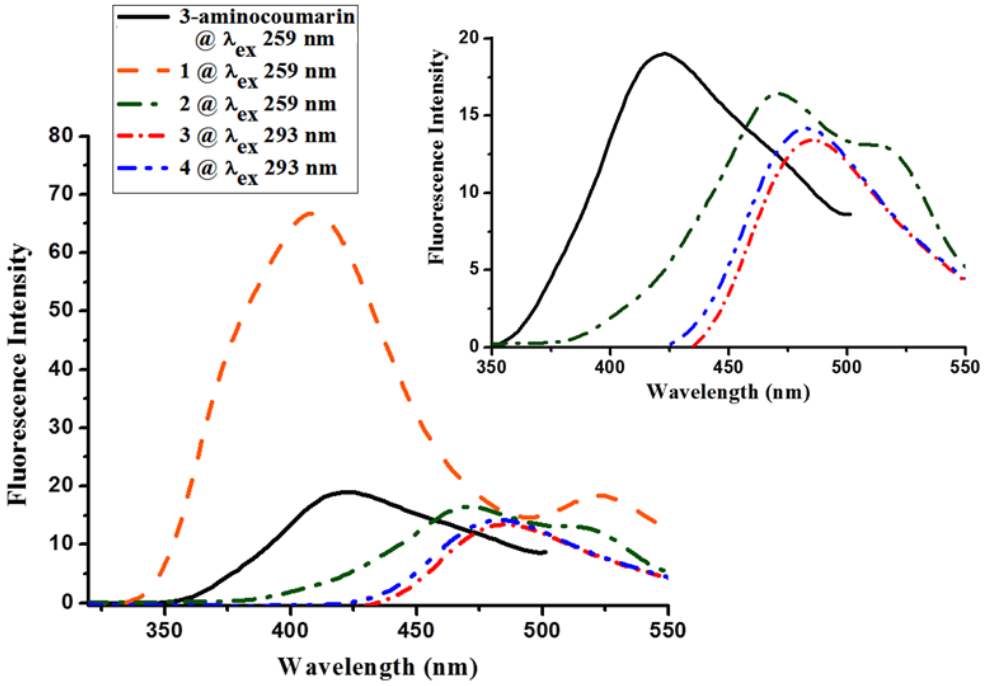

Fig. 2. Fluorescence spectra of 3-amino coumarin and bis-dithiocarbamate metal complexes
at room temperature in 10^{-5} M DMSO solution.

3A.2.6. Geometry optimization of complex 1

The geometry of the complex **1** was optimized on B3LYP/6-31G(d, p) / lanL2DZ level using Gaussian 03 series of programs [31] and the optimized structure is shown in Fig. 3.

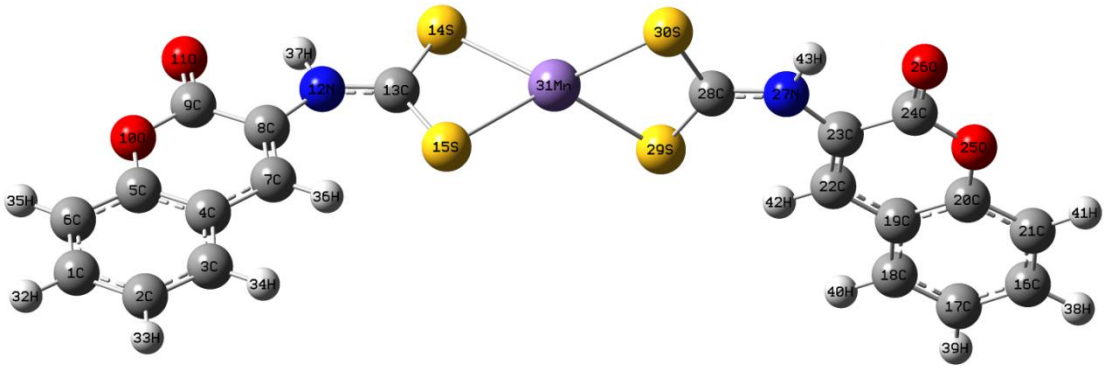

Fig. 3. Optimized geometry of complex 1 at the B3LYP/6-31G(d, p) / lanL2DZ level (**(**E_{opt}: -1.8050 x10^6 kcal/mol).

In the optimized structure, the 3-dithiocarbamato coumarin ligand acts as a monobasic bidentate and coordinates via the sulfur atoms forming two four-membered chelating rings around the Mn(II) centre. These four-membered chelate rings are almost orthogonal to each other as evidenced by the calculated dihedral angle (89.52°) between the least squares planes through these rings (Fig. 4).

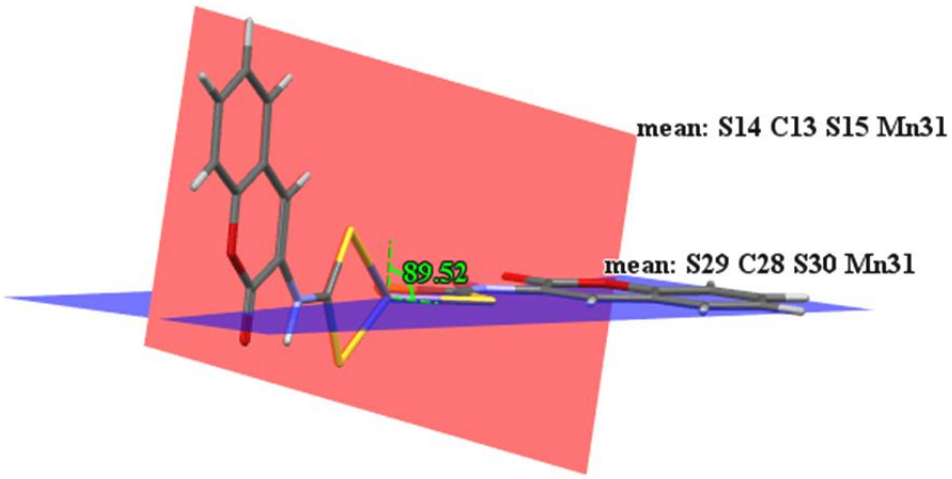

Fig. 4. Dihedral angle between the least squares planes through two chelate rings of **1**.

Further the two C–S bond lengths in each chelate rings are not same, however the calculated geometrical parameters (Table 2) for complex **1** is comparable with the recently reported theoretical [32] and experimental data [33] for Mn(II) dithiocarbamate complexes. The HOMO and LUMO orbitals and their corresponding energies are shown in Fig. 5. The calculated HOMO-LUMO gap of 333.26 nm is comparable with the experimental λ_{max} = 326 nm for **1** which further validates the optimized structure. The theoretical data clearly suggest a distorted tetrahedral geometry around Mn(II) centre.

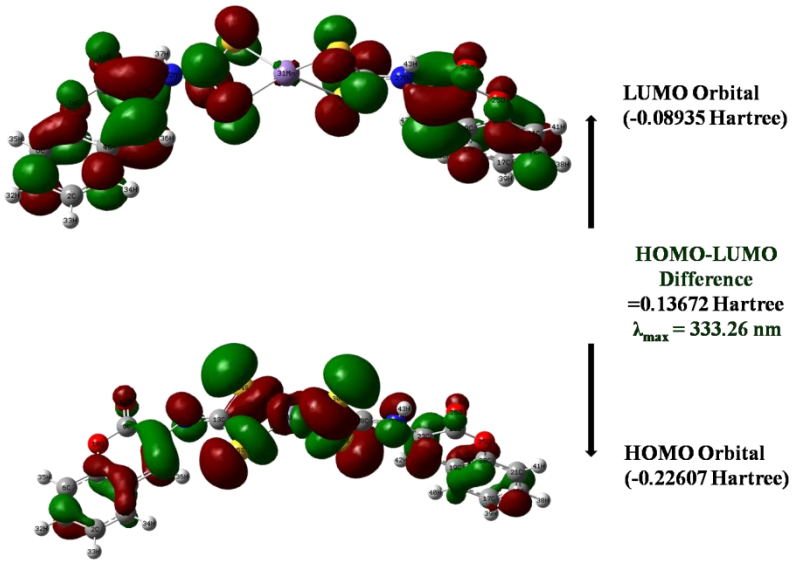

Fig. 5. HOMO-LUMO gap calculated at B3LYP/6-31G(d, p) / lanL2DZ level for complex **1**. a: HOMO = -0.22607 Hartree b: LUMO = -0.08935 Hartree. Calculated HOMO-LUMO gap = 333.26 nm; Experimental λ_{max} = 326 nm.

Table 2. Selected structural parameters for complex **1**

Bond Length (Å)		**Bond Angle (º)**	
Bonds	Distance (Å)	Bonds	Angle (º)
C23–N27	1.400	C8–N12–C13	133.66
N27–C28	1.350	N12–C13–S14	115.97
C28–S29	1.728	N12–C13–S15	123.45
C28–S30	1.740	S14–C13–S15	120.58
N12–C8	1.400	S14–Mn31–S15	74.03
N12–C13	1.350	C23–N27–C28	133.66
C13–S14	1.740	N27–C28–S29	123.45
C13–S15	1.728	N27–C28–S30	115.97
S14–Mn31	2.486	S29–C28–S30	120.58
S15–Mn31	2.516	S29–Mn31–S30	74.03
S29–Mn31	2.516	S14–Mn31–S30	133.44
S30–Mn31	2.486	S15–Mn31–S29	126.34

3A.2.7. Cyclic voltammetric study

The redox behaviour of the Mn^{II} -bis-(3-dithiocarbamato coumarin) complex **1** was studied in the potential range of 0.0 to 2.0 V. The cyclic voltammogram shown in the following figure clearly suggests that the complex **1** is electroactive with respect to the metal center and exhibited two single-electron oxidation waves at Ep_{aI} and Ep_{aII} at 1.046 V and 1.427 V corresponding to $Mn^{II} \rightarrow Mn^{III} + e^-$ and $Mn^{III} \rightarrow Mn^{IV} + e^-$ oxidations, respectively.

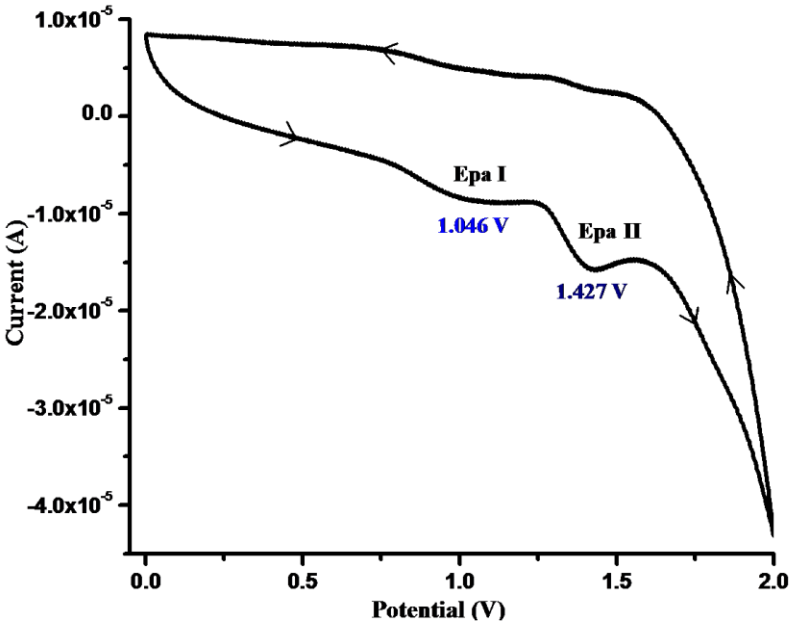

Fig. 6. Cyclic voltammogram for Mn^{II} -bis-(3-dithiocarbamato coumarin) complex **1.**

However the absence of their complementary cathodic peaks suggests an irreversible oxidation of complex **1** which is consistent with the behaviour of $Mn[Pyrr(dtc)]_2$ [34]. This provides a strong evidence for the existence of Mn^{II}-bis-(3-dithiocarbamato coumarin) complex **1**. The formation of $Mn(R_2dtc)_4$ species has been verified electrochemically by A. R. Hendrickson *et al* [34] in solution. The appearance of oxidation waves at more anodic potentials than electrochemically characterized $Mn(Pyrr(dtc))_3]^-$ species suggests that a higher potential is required to oxidize the Mn^{II} center of complex **1** as compared to the Mn^{II} center present in $[Mn(Pyrr(dtc))_3]^-$ species which are indeed much more soluble.

In the present system, the Mn^{II} state could be stabilized by 3-dithiocabamato coumarin ligand because the -N atom of dithiocarbamate moiety is in conjugation with pi-system of enamine and enamine nitrogen is generally electron deficient and thus the possibility of an additional pi-electron flow from nitrogen to sulfur of dithiocarbamate moiety is less. This effect may results into low electron density at the metal centre, preventing the metal from its easy oxidation. This is clearly reflected by the relatively higher oxidation potentials observed in the electrochemical investigation of complex **1** than other Mn^{II} bis-dtc complexes reported elsewhere. This could be the probable reason for unusual behaviour of Mn^{II} -bis-(3-dithiocarbamato coumarin) complex **1**.

3A.2.8. Thermogravimetric study

The thermal properties of the complexes were studied in the temperature ranges from room temperature to 750 ºC. The heating rate was suitably controlled at 10º C min^{-1} under nitrogen atmosphere. The temperature ranges and percentage mass losses during the decompositions as well as the temperature corresponding to the maximum rate of decomposition and the theoretical percentage mass losses are summarized in Table 2. The thermogravimetric plots for the ligand precursor 3-amino couamrin and Mn(II) **1,** Co(III) **2**, Zn(II) **3** and Cd(II) **4** complexes are shown in Fig. 3. A single or multi stage mass loss for these compounds was observed with DTG and corresponding DTA peaks which are attributed to endothermic and/or exothermic elimination of molecular fragments due to the thermal degradation.

The thermogravimetric study of the ligand precursor 3-amino couamrin suggests the total destruction of the molecules up to 220 ºC in two stages. An insignificant mass loss (<1%) was observed on the TG curve at 40.4 ºC (probably due to loss of solvent impurities). The appearance of a sharp endothermic peak at 138.4 ºC on DTA curve without any significant mass loss on DTG curves suggests the occurrence of phase change due to melting of 3-amino coumarin. Practically, the major decomposition stage is accompanied by a mass loss of 90 % which begins at 150 °C and terminates at ~ 225 °C with the maximum rate of decomposition at 214.4 ºC as evidenced by DTG curve. The observed mass loss corresponds to the destruction of the ligand precursor giving behind residues, probably corresponds to the char. In the case of Mn(II) complex **1**, the thermal decompositions are essentially taking place in three stages as evident by the appearance of three peaks on DTG curve. In the first stage 5.9% of mass loss was observed which begins with a rate of 0.116 mg min^{-1} at 77.8 °C on DTG curves and may be attributed to the initial loss of O_2 molecule. After this, mass loss continues up to 750 °C and an overall 57.2 % of loss was observed on TG curve. Due to continuous mass loss observed even at 750 °C the exact mechanism of the fragmentation patterns could not be established. There were some small endothermic peaks observed at 75.9 °C, 188.0 °C and a broad peak at 289.7 °C on DTA curves whereas the maximum rate of mass loss was observed at 287.5 ^{0}C on DTG curve. The thermal degradation of Co(III) **2** complex is taking place in two stages as evident by the appearance two peaks on DTG curves and two endothermic peaks on DTA. In the first stage, an insignificant mass loss (1.5%) was observed on the TG curve probably

due to loss of solvent impurities however it could not be verified from the analytical data. Thereafter, a continuous mass loss of 82.8 % was observed on TG curve with the maximum rate of decomposition of 0.283 mg min^{-1} observed on DTG curve at 233.1°C. Interestingly, the remaining mass of 17.2 % is stable after 700 °C which is in good agreement with the CoS being a final degradation product (theoretical 17.13 %). Furthermore, appearance of two peaks on DTG curves along with two endothermic peaks on DTA curves confirms the two stages of mass loss for the Zn(II) complex **3** which is essentially taking place in the range from 150-700 °C. In the first stage, 11.5% of mass loss was observed with a rate of 0.239 mg min^{-1} at 228.4 °C on DTG curves which may be attributed to the initial loss of acetic acid formed during degradation process. After this, a continuous mass loss of 56.8 % was observed up to 700 °C and an overall 78.3 % of loss was observed on TG curve with the maximum rate of decomposition of 1.109 mg min^{-1} observed on DTG curve at 288.0 °C. In this case also, the remaining mass of 21.7 % is stable after 700 °C which is close to the ZnS (theoretical 18.17 %). In contrast to the degradation patterns observed for **1-3**, Cd(II) **4** complex exhibits one exothermic peak along with two endothermic peaks on DTA curve. Evidently the thermal degradation of complex **4** is taking place in three stages. The first stage of mass loss of 5.5 % on TG curve is attributed to the loss of O_2 molecule during degradation with a very slow rate of degradation 0.09 mg min^{-1} observed on DTG curve. After this a rapid mass loss of 54.4 % was observed in the temperature range of 220-460 °C with the maximum rate of decomposition 1.165 mg min^{-1}. Relatively the final stage is slow and a mass loss of 13.5 % was observed on TG curve with a rate of 0.176 mg min^{-1}, revealed by DTG curve. This mass loss is attributed to the loss of CS_2 (calc. 13.01 %) during decomposition. Interestingly, the remaining mass of 26.6 % is very close to the CdS, being formed as a stable product (theoretical 24.73 %).

It may be noted that the thermal data of complexes **1-3** are in contrast to the literature report where a thermal decomposition of several dithiocarbamate transition metal(II) complexes [35] proceeds in several stages involving many exothermic processes, however, the literature data are consistent with the complex **4**. The endothermic peak temperatures in the complexes **1-3** correspond to the highest weight loss whereas exothermic peak temperature corresponds to the highest weight loss for complex **4** in the thermo grams. These weight losses are mainly associated with

decomposition of the ligand moiety and in case of complexes **2-4**, a subsequent formation of the respective metal sulphides was observed. It is evident from the thermo gram (Fig. 7) that the mass loss during the first stage is depending on the nature of metal ions (Fig. 7). The Mn(II) complex has the least thermal stability and stability trend of the complexes could be said to follow: Mn(II) < Cd(II) < Co(III) < Zn(II).

The thermal analysis data suggest that the complexes **2-4** may be potentially useful as single source precursor for the formation of metal sulphide nano particles [5-6, 8].

Table 3. Thermogravimetric data for ligand precursor 3-amino coumarin and its metal complexes **1–4**.

Entry	Steps	Temp. range (°C)	Weight loss (%)	DTA peak (°C)	DTG peak (°C)	Rate of decomposition (mg min^{-1})	Residue (%) calculated (found)	Final product
3-amino-coumarin	I	40-100	petty	--	40.4	0.13	--	--
	--	--	--	134.8	--	--		
	II	120-220	90.0	215.9	214.4	0.427		
1	I	30-110	5.9	75.9	77.8	0.116	Mass loss continues even after 750 °C	--
	II	111-750	51.2	188.0	188.7	0.128		
				289.7	287.5	0.252		
2	I	100-750	82.8	196.4	201.1	0.260	17.13 (17.2)	CoS
				227.7	233.1	0.283		
3	I	170-230	11.5	227.7	228.4	0.239	18.17 (21.7)	ZnS
	II	231-750	66.8	284.2	288.0	1.109		
4	I	80-220	5.5	244.7	191.1	0.090	24.73 (26.6)	CdS
	II	221-460	54.4	274.9	245.4	0.487		
	III	461-750	13.5	455.1	278.2	1.165		
					453.6	0.176		

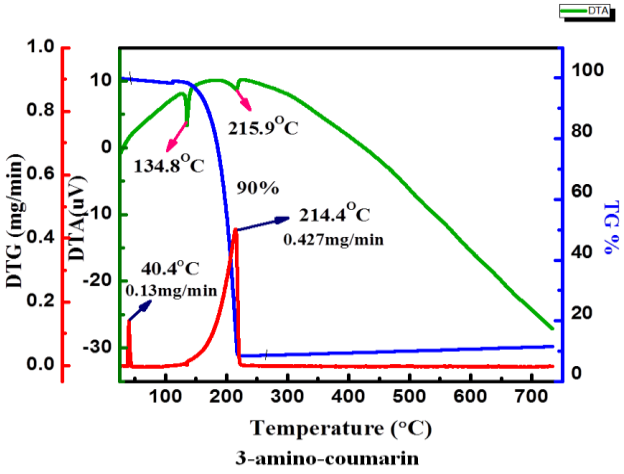

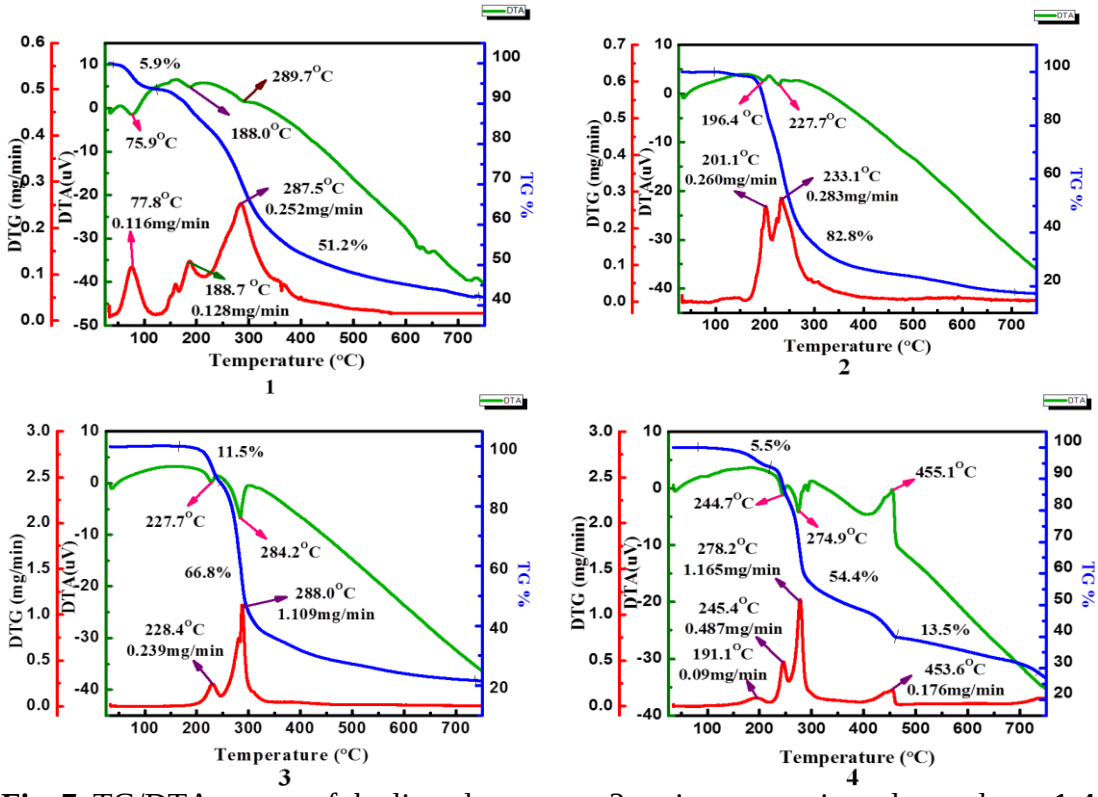

Fig. 7. TG/DTA curves of the ligand precursor 3-amino coumarin and complexes **1-4**.

3A.2.9. Optical band gap

The absorption of complexes **1-4** in the visible range of the solar spectrum indicates that these compounds may act as a photosensitizer for wide band-gap semiconductors. Thus we have further investigated their optical behaviour towards wide band-gap semiconductors with the help of UV-vis transmittance measurements. The value of the optical energy band gap was obtained from the photon absorption corresponding to electronic excitation from the valence band to the conduction band.

The optical absorption coefficient (α) was obtained from the transmittance spectrum of **1-4** by using the formula: $\alpha = \frac{1}{d}\ln\left[\frac{1}{T}\right]$, where, d is thickness of the sample and T is the transmittance. The well known Davis and Mott equation [36] is used to determine the relation between the absorption coefficients α and the incident photon energy (hν). In order to determine optical band gap of the complexes **1-4**, we applied the models for both direct and indirect transitions. For this, the $(\alpha h\nu)^2$ (direct transition) and $(\alpha h\nu)^{1/2}$ (indirect transitions) versus hν were plotted for each complexes. Evidently the absorption in the samples corresponds to a direct energy gap. A plot of $(\alpha h\nu)^{1/\gamma}$ versus hν (Fig. 8) for each complex was drawn with γ = 1/2 (direct allowed transition) to calculate the band gap energy [37]. This gives a direct

band gap by extrapolating the linear part of the plot. The calculated band gap energies (Eg) for **1–4** fall in the range of 2.039-2.565 eV which suggest that compounds 1–4 display the feature of a direct band gap semiconductor. This could attract the researchers working in the fields of optical communication and optical devices. The lower values of band gap energies for these complexes are obvious, as dithiolato complexes are widely explored as semiconducting materials [1f].

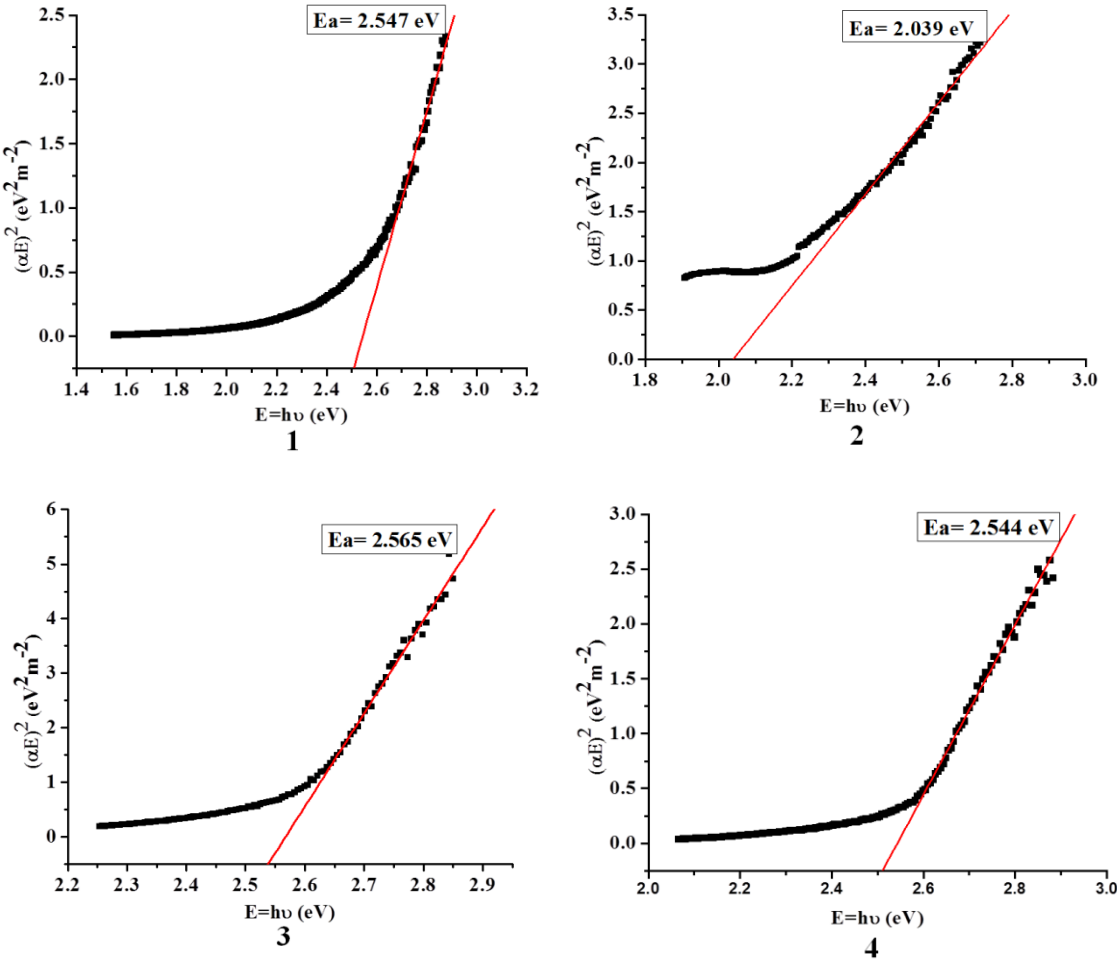

Fig. 8. A plot of $(\alpha E)^2(eV^2m^{-2})$ versus hυ (eV) for the complexes **1-4**.

3A.3. Conclusion

In conclusion, a novel series of neutral monometallic dithiocarbamate complexes of Mn(II) **1**, Co(II) **2**, Zn(II) **3** and Cd(II) **4** has been prepared from 3-amino coumarin, CS_2 and corresponding metal acetates in a single step. All the complexes are characterized by standard spectroscopic methods. The spectroscopic and magnetic data suggest a tetrahedral/ distorted tetrahedral geometry around Mn(II), Zn(II), Cd(II) and octahedral geometry around the Co(III) centres. All the complexes

exhibit bathochromic shifts of the intra-molecular (CT→M) charge-transfer emissions in their fluorescence spectra. Interestingly, the thermogravimetric study performed on the complexes **1-4** indicates that complexes **2-4** may be suitably used as a single source material for the preparation of metal sulphide nano particles. Furthermore the calculated band gap energies (Eg) fall in the range of 2.039-2.565 eV, suggesting a feature of direct band gap semiconducting nature of **1-4**.

3A.4. Experimental section

3A.4.1. Materials and measurement

All solvents were purchased from the commercial sources and were freshly distilled prior to use. Reagents such as metal acetates $Mn(OAc)_2.4H_2O$, $Co(OAc)_2.4H_2O$, $Zn(OAc)_2.2H_2O$, $Cd(OAc)_2.2H_2O$ and CS_2 were purchased from Merck and these were used without further purification. All the reactions and manipulations were performed under an inert atmosphere. The starting precursor 3-amino coumarin was synthesized by using literature procedure [11c] and characterized well prior to use. Elemental analyses (C, H, N) were carried out on a Perkin-Elmer 2400 analyzers. ESI MS spectra were recorded on Bruker instrument micrOTOF-Q II. Dart-MS analysis of one sample was performed on JEOL-AccuTOF JMS-T100LC mass spectrometer. FT-IR (KBr pellets) spectra were recorded in the 4000-400 cm^{-1} range using a Perkin-Elmer FT-IR spectrometer. The ^{1}H and ^{13}C NMR spectra of relevant complexes were obtained on a Bruker AV-III 400 MHz spectrometer in DMSO-d_6. UV-visible spectra were recorded on a Perkin Elmer Lambda 35 UV-visible spectrophotometer and the optical characterization of solid samples was performed by using the UV-visible transmittance measurements. Magnetic moments were obtained by using Faraday Valance-2002 (1.0Tesla), balance-Mettler UMx5, at room temperature. Fluorescence was recorded on JASCO make spectrofluorometer model FP-6300. TGA/DTA plots were obtained using SII TG/DTA 6300 in flowing N_2 with a heating rate of 10 °C min^{-1}. Cyclic voltammetric study was performed on a CH Instruments 600C potentiostat, using a Pt disk as the working electrode, Ag/AgCl as the reference electrode and a Pt wire as the counter electrode. Cyclic voltammetric study was carried out using 1.0 mM solution of the complex **1** in 0.1 M tetra-n-butylammonium tetrafluoroborate (Bu_4NBF_4) in CH_2Cl_2

with a scan rate of 300 mVs^{-1}. The measurements were carried out at room temperature (25 ºC).

3A.4.2. Synthesis of monometallic [M(1,1-dithiolato)$_n$] (1–4)

3-Amino coumarin (100 mg, 0.621mmol) and an excess amount of CS_2 (0.5 mL, 7.452 mmol) were taken in a single necked flask containing 10 mL of Et_3N. The reaction mixture was stirred rigorously for two hours at room temperature. During these hours, a change in colour from colourless to pale yellow was observed, indicating the formation of 3-dithiocarbamato coumarin ligand. This ligand was allowed to react *in situ* with $Mn(OAc)_2.4H_2O$ (76.10 mg, 0.310 mmol), $Co(OAc)_2.4H_2O$ (77.34 mg, 0.310 mmol), $Zn(OAc)_2.2H_2O$ (68.15 mg, 0.310 mmol) or $Cd(OAc)_2.2H_2O$ (82.75 mg, 0.310 mmol) respectively over a period of 14 hours. A colour change from light yellow to golden yellow and light yellow to green were observed during the formation of complex **1** and **2** whereas a colour change from light yellow to dark yellow were seen during the formation of **3** and **4**. Except Mn (II), all the reactions gave a sticky precipitate which was purified by column chromatography using 25% (v/v) ethyl acetate/ petroleum ether solvent mixture as eluent. In case of Mn(II), the reaction mixture was filtered and the free flowing residue was washed several times with petroleum ether followed by diethyl ether and finally dried under vacuum to yield the product.

[Mn(1,1-dithiolato)$_2$] (1). Golden yellow solid: Yield (%): 70. M.p. (°C): 225. Formula (F.W.) (g mol^{-1}): $C_{20}H_{12}N_2O_4S_4Mn$ (527). Anal. Calcd for **1:** C, 45.54; H, 2.29; N, 5.31; S, 24.31. Found: C, 45.28; H, 2.34; N, 5.71; S, 24.21. %. IR (KBr, in cm^{-1}): 3330(br, s), 3040(w), 1719(vs), 1565(br, s), 1418(br, s), 1342(w), 1284(w), 1225(m), 1191(w), 1124(w), 1062(w), 1027(m), 933(m), 755(m), 664(m). ESI-MS (positive ion mode, CH_3CN): *m/z* = 529.27 $[M+2H]^+$). μ_{eff} (298 K): 6.78 B.M.

[Co(1,1-dithiolato)$_3$] (2). Green solid: Yield (%): 25. M.p. (^oC): 168. Formula (F.W.) (g mol^{-1}): $C_{30}H_{18}N_3O_6S_6Co$ (766.9). Anal. Calc. for **2**: C, 46.93; H, 2.36; N, 5.47; S, 25.06. Found: C, 47.25; H, 2.54; N, 5.18; S, 25.74%. IR (KBr, in cm^{-1}): 3245(br, w), 3069(w), 2972(w), 2926(w), 1713(vs), 1628 (sh), 1603(m), 1511(s), 1485(sh), 1455(sh), 1365(s), 1318(s), 1187(m), 1101(m), 1015(m), 923(w), 883(w), 754(s). ^1H NMR (400 MHz, $CDCl_3$): δ, ppm: 9.37 (s, 1H, N-*H*); 9.12 (s, 1H, N-*H*); 9.06 (s, 1H,

N-*H*); 7.62-7.41 (m, 3H, *Ph*); 7.34-7.31 (m, 12H, *Ph*); ^{13}C NMR (400 MHz, $CDCl_3$): *δ*, ppm: 208.04, 203.27 (-NCS_2), 158.16, 150.21, 150.11, 130.65, 130.37, 130.15, 128.11, 127.84, 127.76, 125.56, 125.46, 125.33, 123.83, 123.68, 121.97, 121.62, 118.98, 118.78, 116.66, 116.60 (Ph). ESI-MS (positive ion mode, CH_3CN): *m/z* = 531.95 $[M+H]^+$).

[Zn(1,1-dithiolato)$_2$] (3). Dark yellow solid: Yield (%): 40. M.p. (^{o}C): 272. Formula (F.W.) (g mol^{-1}): $C_{20}H_{12}N_2O_4S_4Zn$ (535.9). Anal. Calcd for **3:** C, 44.65; H, 2.25; N, 5.21; S, 23.84. Found: C, 44.72; H, 2.31; N, 5.28; S, 23.74. %. IR (KBr, in cm^{-1}): 3315(br, s), 3046(w), 1728(br, s), 1643(s), 1604(s), 1536(s), 1474(br, s), 1389(br, s), 1247(br, s), 1179(s), 1126(w), 928(s), 874(m), 756(s), 648(s). ^{1}H NMR (400 MHz, DMSO-d_6): *δ*, ppm: 9.078 (s, 2H, N-*H*); 8.447 (s, 2H, *Ph*); 7.88-7.86 (dd, 1H, *Ph*); 7.79-7.72(m, 2H, *Ph*); 7.58-7.54 (dd, 1H, *Ph*); 7.50-7.35 (m, 1H, *Ph*); 7.29-7.21 (m, 1H, *Ph*); 6.93-8.87 (m, 2H, *Ph*). ^{13}C NMR (400 MHz, DMSO-d_6): *δ*, ppm: 176.85 (s, 2C, -NCS_2), 163.93, 157.23, 153.44, 145.77, 133.89, 132.04, 131.32, 129.76, 126.69, 125.85, 120.36, 119.82, 118.40, 116.96, 116.35, 110.71. Dart-MS (positive ion mode): *m/z* = 537.28 $[M+H]^+$).

[Cd(1,1-dithiolato)$_2$] (4). Dark yellow solid: Yield (%): 35. M.p. (^{o}C): 278. Formula (F.W.) (g mol^{-1}): $C_{20}H_{12}N_2O_4S_4Cd$ (584). Anal. Calcd for **4:** C, 41.06; H, 2.07; N, 4.79; S, 21.93. Found: C, 41.16; H, 2.11; N, 4.85; S, 21.73 %. IR (KBr, in cm^{-1}): 3316(br, s), 3047(w), 2426(w), 1723(s), 1642(m), 1606(m), 1537(m), 1474(s), 1383(vs), 1242(m), 1179(s), 1132(w), 925(w), 756(s). ^{1}H NMR (400 MHz, DMSO-d_6): *δ*, ppm: 9.063 (s, 2H, N-*H*); 8.436 (s, 2H, *Ph*); 7.88-7.85 (dd, 1H, *Ph*); 7.79-7.71(m, 1H, *Ph*); 7.59-7.55 (dd, 1H, *Ph*); 7.50-7.43 (m, 1H, *Ph*); 7.40-7.36 (m, 1H, *Ph*); 7.29-7.21 (m, 1H, *Ph*); 6.932-8.89 (m, 2H, *Ph*). ^{13}C NMR (400 MHz, DMSO-d_6): *δ*, ppm: 176.95 (s, 2C, -NCS_2), 163.82, 157.24, 153.51, 145.92, 134.02, 132.14, 131.24, 129.86, 125.94, 120.27, 119.90, 119.72, 118.44, 117.04, 116.42, 116.30, 110.61. ESI-MS (positive ion mode, CH_3CN): *m/z* = 584.35 $[M]^+$).

3A.5. References

1. (a) Hogarth, G. *Prog. Inorg. Chem*. **2005**, *53*, 71; (b) Tiekink, E. R. T.; Haiduc, I. *Prog. Inorg. Chem*. **2005**, *54*, 127; (c) Bond, A. M.; Hendrickson, A. R.; Martin, R. L.; Moir, J. E.; Page, D. R. *Inorg. Chem.* **1983**, *22*, 3440; (d) Kobayashi, A.; Fujiwara, E.; Kobayashi, H. *Chem. Rev*. **2004**, *104*, 5243; (e) Bousseau, M.;

Valade, L.; Legros, J. P.; Cassoux, P.; Garbaukas, M.; Interrante, L. V. *J. Am. Chem. Soc.* **1986**, *108*, 1908; (f) Coomber, A. T.; Beljonne, D.; Friend, R. H.; Bredas, J. L.; Charlton, A.; Robertson, N.; Underhill, A. E.; Kurmoo, M.; Day, P. *Nature* **1996**, *380*, 144; (g) Singh, N.; Singh, V. K. *Int. J. Inorg. Mat*. **2000**, *2*, 167.

2. (*a*) Singh, N.; Kumar, A.; Prasad, R.; Molloy, K. C.; Mahon, M. F. Dalton Trans. **2010**, *39*, 2667; (*b*) Wilton-Ely, J. D. E. T.; Solanki, D.; Knight, E. R.; Holt, K. B.; Thompson, A. L.; Hogarth, G. Inorg. Chem. **2008**, *47*, 9642; (*c*) Wilton-Ely, J. D. E. T.; Solanki D.; Hogarth, G. Eur. J. Inorg. Chem., **2005**, 4027; (*d*) Trindade, T.; O'Brien, P.; Pickett, N. L. Chem. Mater. **2001**, *13*, 3843; (*e*) Wong, W. W. H.; Cookson, J.; Evans, E. A. L.; McInnes, E. J. L.; Wolowska, J.; Maher, J. P.; Bishop, P.; Beer, P. D. Chem. Commun. **2005**, 2214.
3. King, J. N.; Fritz, J. S. Anal. Chem. **1987**, *59*, 703.
4. (a) Yoshikawa, Y.; Adachi, Y.; Sukurai, H. Life Sciences **2007**, *80*, 759; (b) Ozkirimli, S.; Apak, T. I.; Kiraz, M.; Yegenoglu, Y. Arch. Pharm. Res. **2005**, *28*, 1213; (c) Shaheen, F.; Badshah, A.; Gielen, M.; Gieck, C.; Jamil, M.; de Vos, D. J. Organomet. Chem. **2008**, *693*, 1117; (d) Alverdi, V.; Giovagnini, L.; Marzamo, C.; Seraglia, R.; Bettio, F.; Sitran, S.; Graziani, R.; Fregona, D. J. Inorg. Biochem. **2004**, *98*, 1117.
5. Fan, D.; Afzaal, M.; Malik, M. A.; Nguyen, C. Q.; Brien, P. O.; Thomas, P. J. Coord. Chem. Rev. 2007, 251, 1878.
6. (a) Trindade, T.; O'Brien, P. Chem. Vap. Deposit. **1997**, *3*, 75; (b) Ajibade, P. A.; Onwudiwe, D. C.; Moloto, M. J. Polyhedron **2011**, *30*, 246; (c) O'-Brien, P.; Walsh, J. R.; Watson, I. M.; Motevalli, M.; Henriksen, L. J. Chem. Soc., Dalton Trans. **1996**, 2491; (d) Green, M.; Prince, P.; Gardener, M. J. Steed, Adv. Mater. **2004**, *16*, 994; (e) Nomura, R.; Seki, Y.; Konishi, K.; Matsuda, H. Appl. Organomet. Chem. **1992**, *6*, 685.
7. (a) Sharma, A. K. Thermochim. Acta, **1986**, *104*, 339; (b) Hill, J. O.; Murray, J. P.; Patil, K. C. Rev. Inorg. Chem. **1994**, *14*, 363.
8. Onwudiwe, D. C.; Ajibade, P. A. Int. J. Mol. Sci. **2011**, *12*, 1964.
9. Memon, A. A.; Afzaal, M.; Malik, M. A.; Nguyen, C. Q.; O'Brien, P.; Raftery, J. Dalton Trans. **2006**, 4499.

10. kumaar, S. S.; Selvi, T. R. Synth. React. Inorg. Met.-Org. Nano-Met. Chem. **2008**, *38*, 710.
11. (a) Yu, T.; Zhang, P.; Zhao, Y.; Zhang, H.; Meng, J.; Fan, D. Org. Electron. **2009**, *10*, 653; (b) Asish, R.; Arunima, M.; Raghunath, S. Tetrahedron Lett. **2010**, *51*, 1099; (c) Kudale, A. A.; Kendall, J.; Warford, C. C.; Wilkins, N. D.; Bodwell, G. J. Tetrahedron Lett. **2007**, *48*, 5077; (d) Yadav, L. D. S.; Singh, S.; Rai, V. K. Tetrahedron Lett. **2009**, *50*, 2208.
12. Kadhum, A. A. H.; Mohamad, A. B.; Al-Amiery, A. A.; Takriff, M. S. Molecules **2011**, *16*, 6969.
13. Osborne, A. G.; Cremlyn, R. J.; Warmsley, J. F. Spectrochim. Acta, Part A **1995**, *51*, 2525.
14. (a) Trivedi, K.; Sethna, S. J. Org. Chem. **1960**, *25*, 1817; (b) Chakravarti, D.; Dutta, S. P.; Mitra, A. K. Curr. Sci. **1965**, 177.
15. Verma, S. K.; Kadu, R.; Singh, V. K. Synth. React. Inorg. Met.-Org. Nano-Met. Chem. **2014**, *44*, 441.
16. Hogarth, G. *Prog. Inorg. Chem.* **2005**, *53*, 71.
17. Coucouvanis, D. In: Progress in Inorganic Chemistry11, Lippard, S. I. Ed., New York: Interscience, 1970.
18. (a) Shyamala, B. S.; Lakshmi, P. V. A.; Raju, V. J. *J. Sci. Res*. **2010**, *2*, 525; (b) Riveros, P. C.; Perilla, I. C.; Poveda, A.; Keller, H. J.; Pritzkow, H. *Polyhedron* **2000**, *19*, 2327; (c) Johnson, B. F. G.; Al-Obalidi, K. H.; Mecleverty, J. A. *J. Am. Chem. Soc. A* **1969**, *19*, 1668; (d) Anderson, R. J.; Bendell, D. J.; Groundwater, P. W. Organic Spectroscopic Analysis; RSC: Cambridge, UK, 2004.
19. Shyamala, B. S.; Lakshmi, P. V. A.; Raju. V. J. J. Sci. Res. **2010**, *2*, 525.
20. Shahid, M.; Ruffer, T.; Lang, H.; Awan, S. A.; Ahmad, S. *J. Coord. Chem*. **2009**, *62*, 440.
21. Kaur, J.; Marwaha, S. S.; Sodhi, G. S. *J. Indian Chem. Soc*. **1999**, *76*, 185.
22. Wong, W. W. H.; Phipps, D. E.; Beer, P. D. *Polyhedron* **2004**, *23*, 2821.
23. Abu-Eitta, R. H.; Bahgat, A. H.; El-Tawil, C. *Can. J. Chem*. **1985**, *63*, 1173.
24. Gölcü, A.; Yavuz, P. *Russ. J. Coord. Chem*. **2008**, *34*, 106.
25. Hogarth, G.; Rainford-Brent, E. J. C. R. C. R.; Kabir, S. E.; Richards, I.; Wilton-Ely, J. D. E. T.; Zhang, Q. *Inorg. Chim. Acta* **2009**, *362*, 2020.
26. Nicolay, I. D.; Maria, K.; Kuduk-Jaworska, J. *Z. Naturforsch. 57b*, **2002**, 1174.

27. Gölcü, A. *Trans. Met. Chem*. **2006**, *31*, 405.
28. Chai, L.-Q.; Wang, G.; Sun, Y.-X.; Dong, W.-K.; Zhao, L.; Gao, X.-H. *J. Coord. Chem*. **201**2, *65*, 1621.
29. Pandey, R.; Kumar, P.; Singh, A. K.; Shahid, M.; Li, P. Z.; Singh, S. K.; Xu, Q.; Misra, A.; Pandey, D. S. *Inorg. Chem*. **2011**, *50*, 3189.
30. Sreedaran, S.; Bharathi, K. S.; Rahiman, A. K.; Jagadish, L.; Kaviyarasan, V.; Narayanan, V. Polyhedron **2008**, *27*, 2931.
31. Frisch, M. J.; Trucks, G. W.; Schlegel, H. B.; Scuseria, G. E.; Robb, M. A.; Cheeseman, J. R.; Montgomery, J. A.; Vreven, Jr. T.; Kudin, K. N.; Burant, J. C.; Millam, J. M.; Iyengar, S. S.; Tomasi, J.; Barone, V.; Mennucci, B.; Cossi, M.; Scalmani, G.; Rega, N.; Petersson, G. A.; Nakatsuji, H.; Hada, M.; Ehara, M.; Toyota, K.; Fukuda, R.; Hasegawa, J.; Ishida, M.; Nakajima, T.; Honda, Y.; Kitao, O.; Nakai, H.; Klene, M.; Li, X.; Knox, J. E.; Hratchian, H. P.; Cross, J. B.; Adamo, C.; Jaramillo, J.; Gomperts, R.; Stratmann, R. E.; Yazyev, O.; Austin, A. J.; Cammi, R.; Pomelli, C.; Ochterski, J. W.; Ayala, P. Y.; Morokuma, K.; Voth, G. A.; Salvador, P.; Dannenberg, J. J.; Zakrzewski, V. G.; Dapprich, S.; Daniels, A. D.; Strain, M. C.; Farkas, O.; Malick, D. K.; Rabuck, A. D.; Raghavachari, K.; Foresman, J. B.; Ortiz, J. V.; Cui, Q.; Baboul, A. G.; Clifford, S.; Cioslowski, J.; Stefanov, B. B.; Liu, G.; Liashenko, A.; Piskorz, P.; Komaromi, I.; Martin, R. L.; Fox, D. J.; Keith, T.; Al-Laham, M. A.; Peng, C. Y.; Nanayakkara, A.; Challacombe, M.; Gill, P. M. W.; Johnson, B.; Chen, W.; Wong, M. W.; Gonzalez, C.; Pople, J. A. *Gaussian, Inc., Wallingford*, CT, **200**4.
32. Beyramabadi, S. A.; Morsali, A.; Vahidi, S. H. *J. Struct. Chem.* **2012**, *53*, 665.
33. (a) Konarev, D. V.; Khasanov, S. S.; Kovalevsky, A. Y.; Lopatin, D. V.; Rodaev, V. V.; Saito, G.; Forró, B. N. L.;. Lyubovskaya, R. N *Cryst. Growth Des*. **2008**, *8*, 1161; (b) Siddiqi, K. S.; Nishat, N. *Synth. React. Inorg. Met.-Org. Chem.* **2000**, *30*, 1505; (c) Khan, S.; Nami, S. A. A.; Siddiqi, K. S. *J. Mol. Struct*. **2008**, *875*, 478.
34. Hendrickson, A. R.; Martin, R. L.; Rohde, N. M. *Inorg. Chem.* **1974**, *13*, 1933.
35. Ali, B. F.; Al-Akramawi, W. S.; Al-Obaidi, K. H.; Al-Karboli, A. H. A. *Thermochim. Acta*. **2004**, *419*, 39.
36. Davis, E. A.; Mott, N. F. *Philos. Mag.* **1970**, *22*, 903.
37. Tauc, J. *J. Mater. Res. Bull*. **1970**, *5*, 721.

3A.6. Spectra

3A.6.1. IR spectra

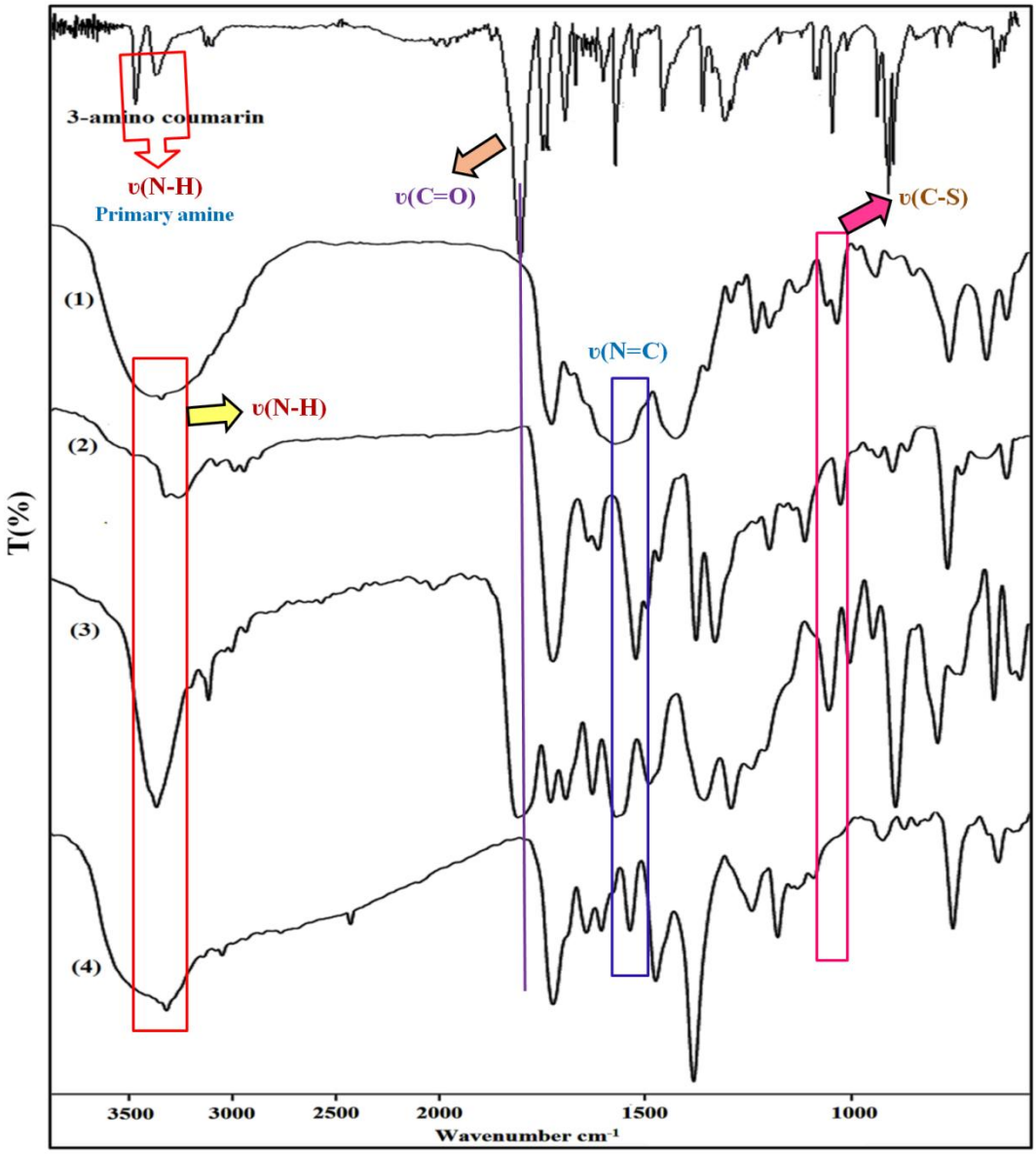

Figure S1. IR spectrum of 3-amino coumarin and its Metal(II) dithiocarbamate complexes **1-4**.

3A.6.2. NMR spectra

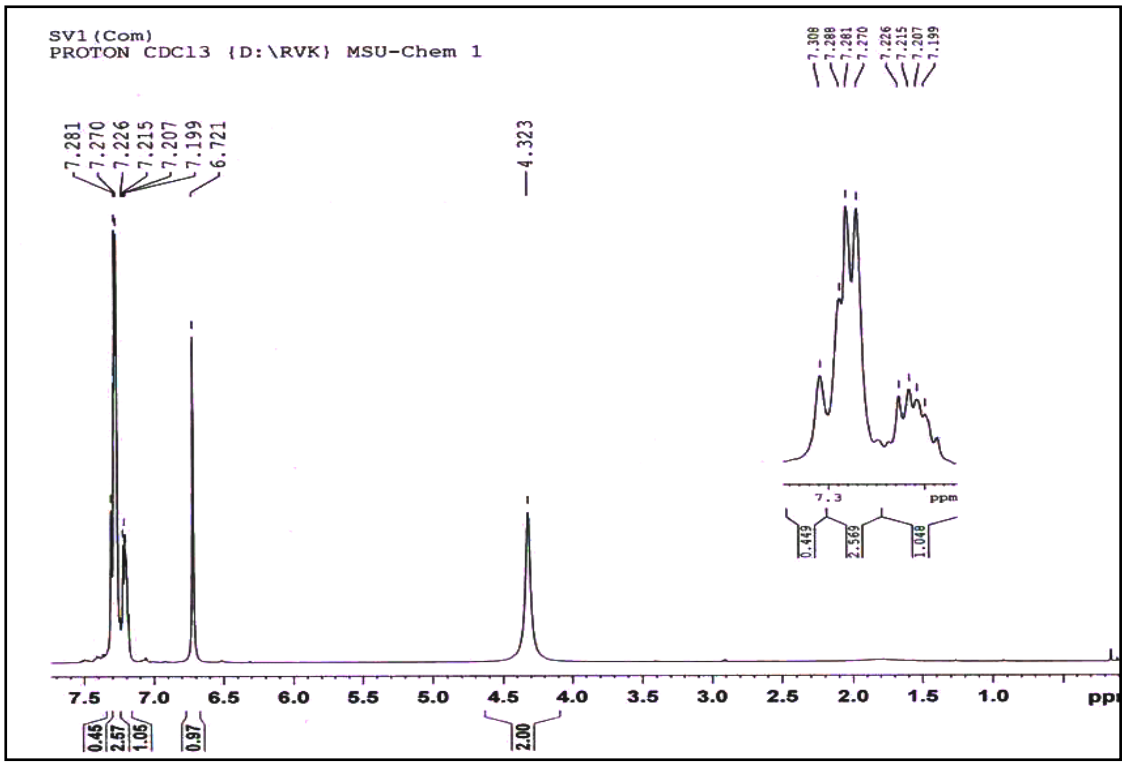

Figure S2. ^{1}H NMR spectrum of 3-amino coumarin.

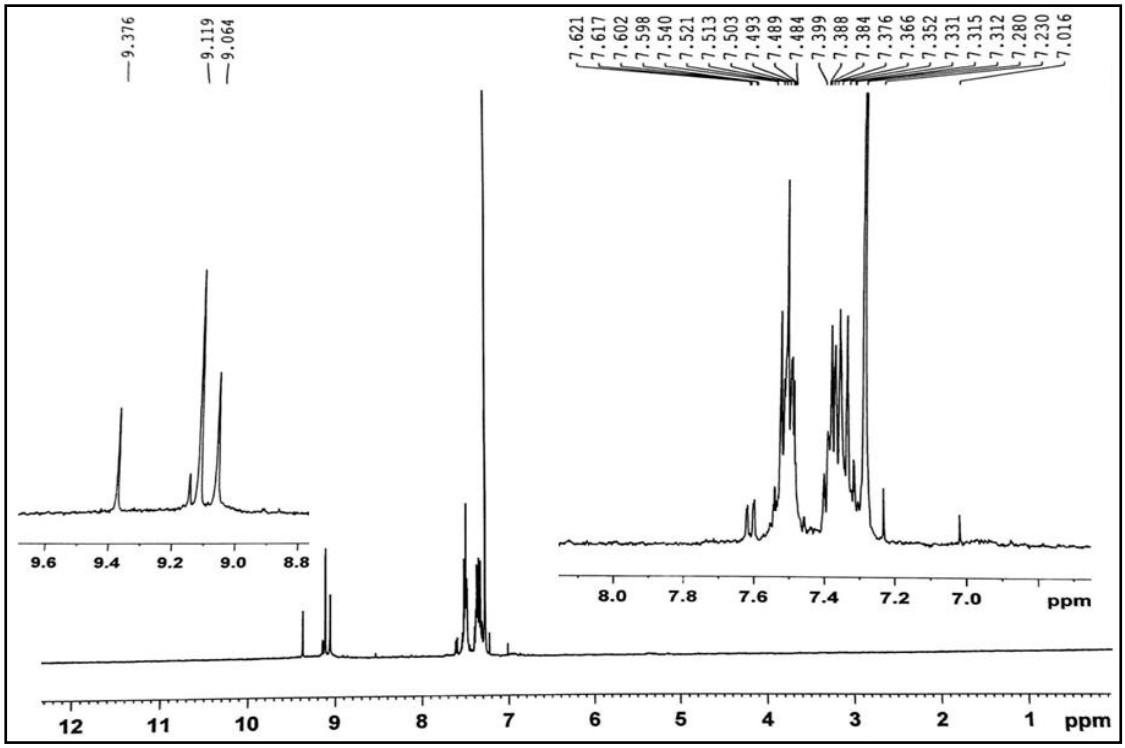

Figure S3. ^{1}H NMR spectrum of $Co^{III}(1,1\text{-ditho})_3$ complex (2)

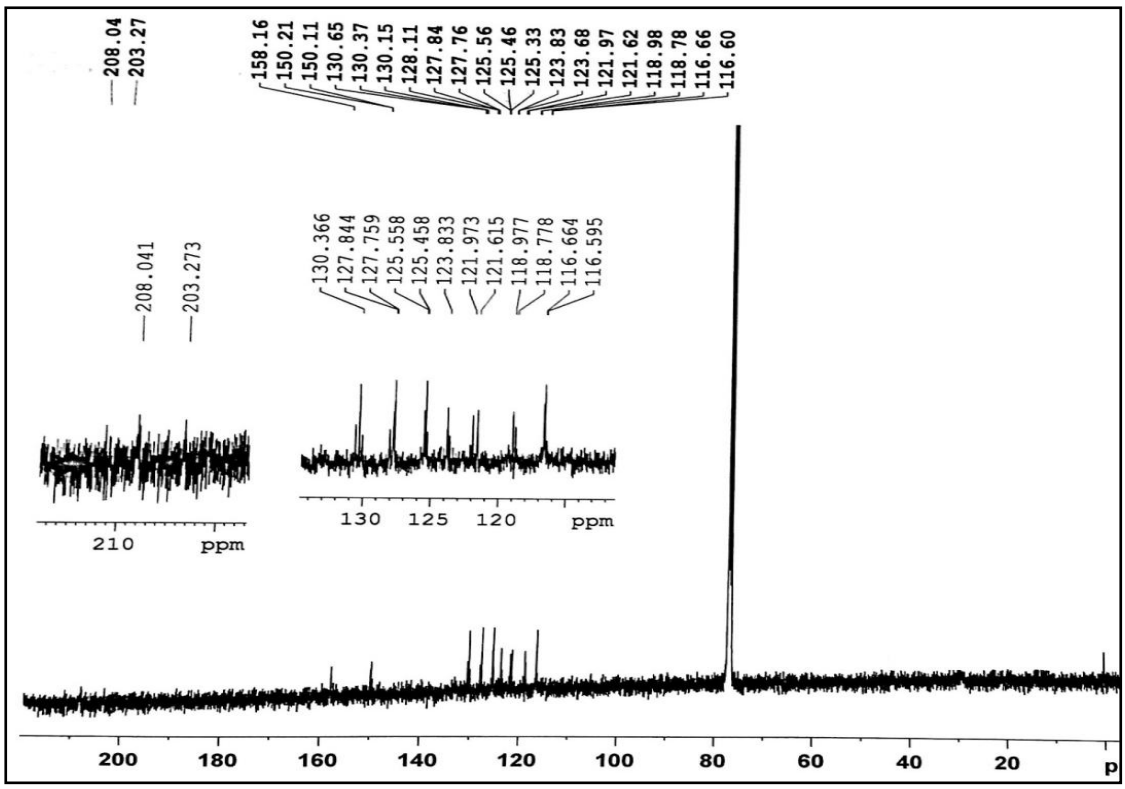

Figure S4. ^{13}C NMR spectrum of $Co^{III}(1,1\text{-ditho})_3$ complex (2)

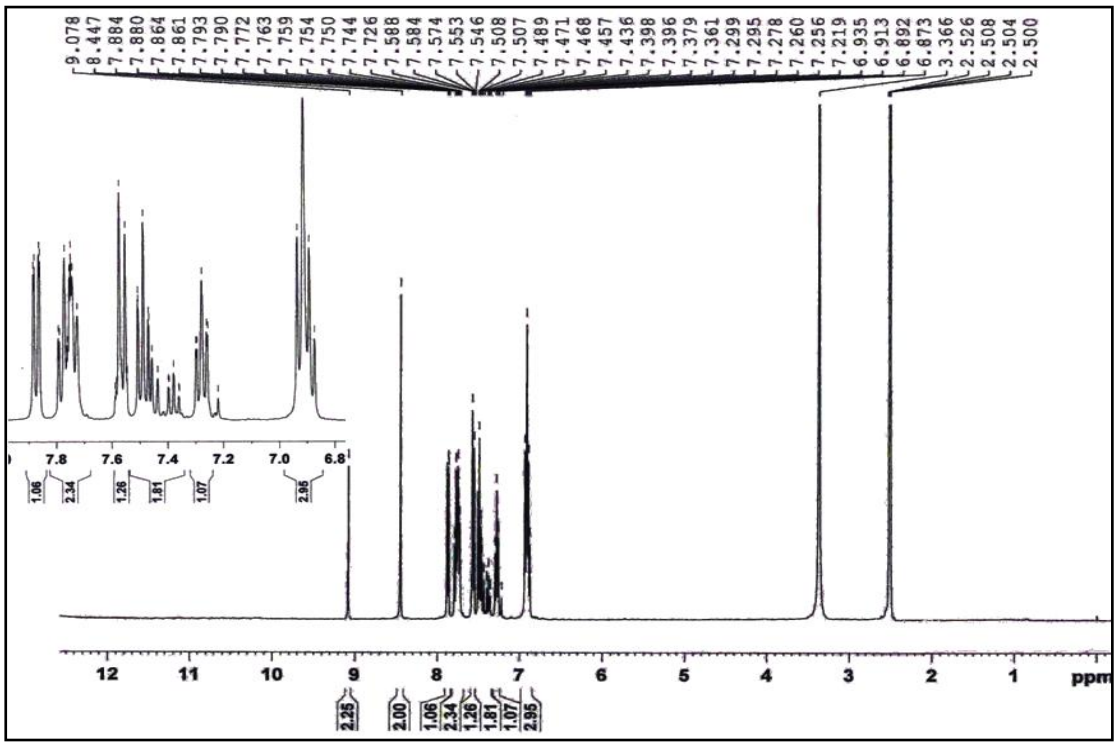

Figure S5. ^{1}H NMR spectrum of Bis-dithiocarbamate Zn(II) complex **3**.

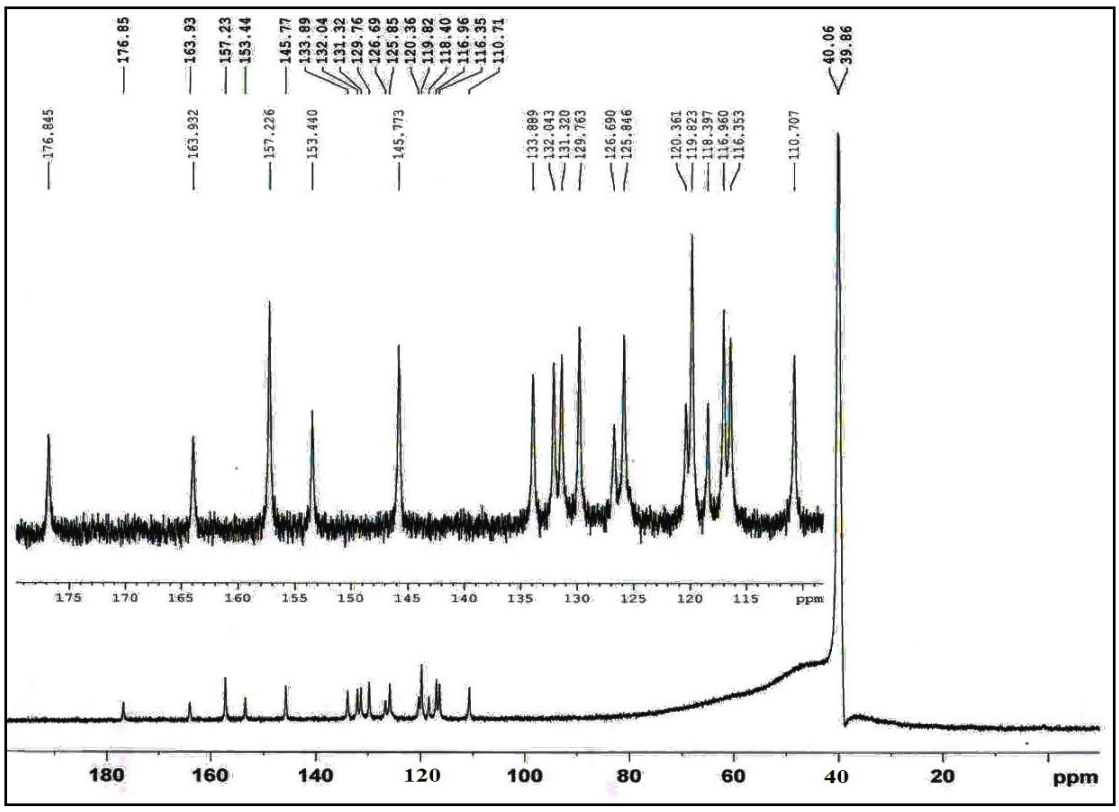

Figure S6. ^{13}C NMR spectrum of Bis-dithiocarbamate Zn(II) complex **3**.

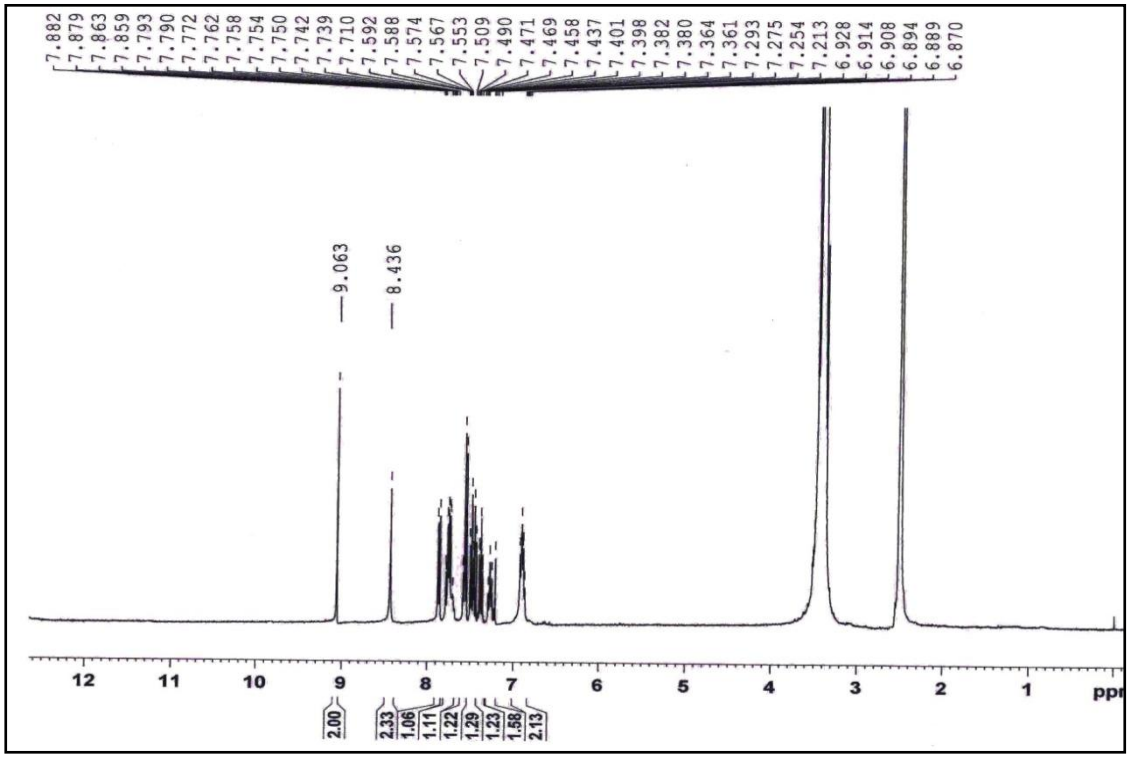

Figure S7. ^{1}H NMR spectrum of Bis-dithiocarbamate Cd(II) complex **4**.

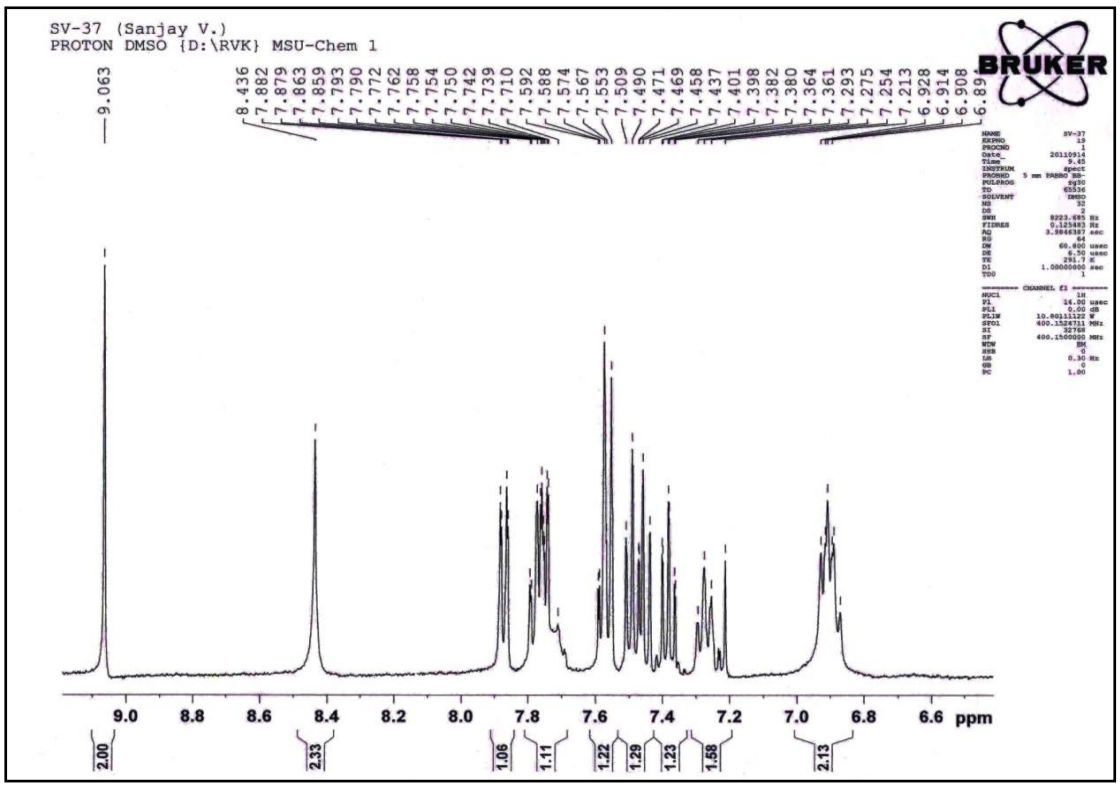

Figure S8. Expansion of ^{1}H NMR spectrum of Bis-dithiocarbamate Cd(II) complex **4**.

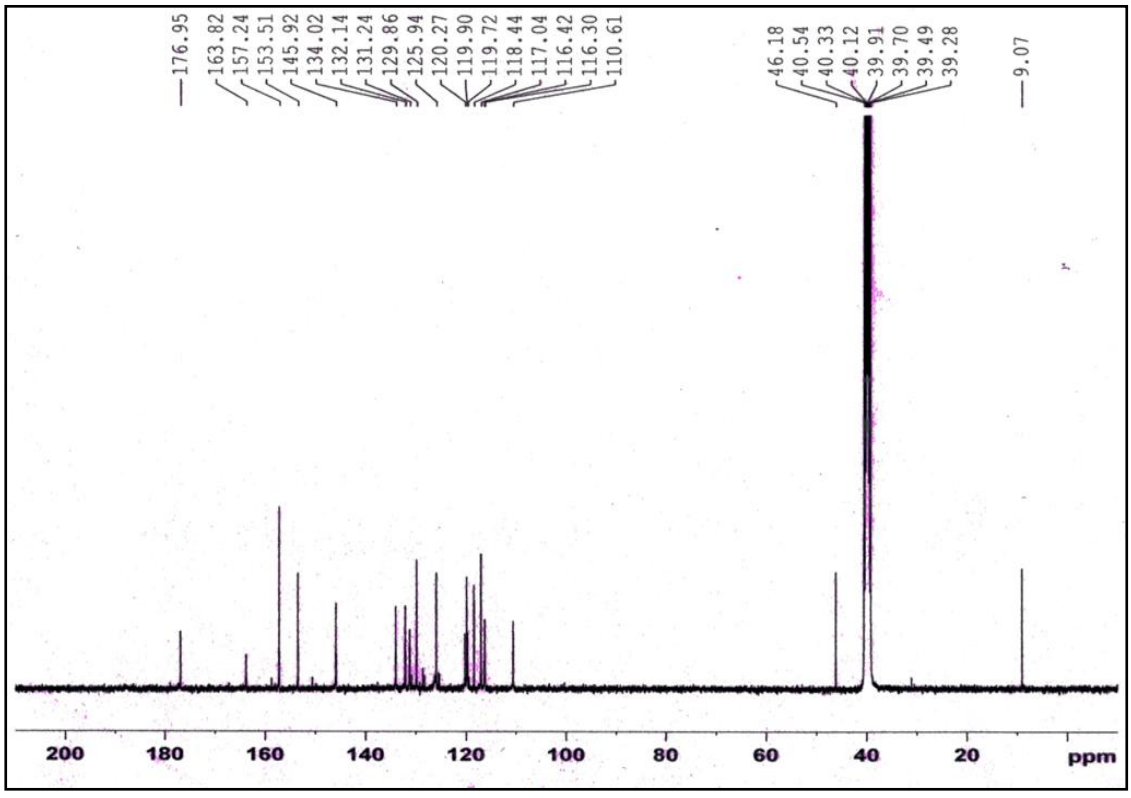

Figure S9. ^{13}C NMR spectrum of Bis-dithiocarbamate Cd(II) complex **4**.

3A.6.3. ESI MS spectra

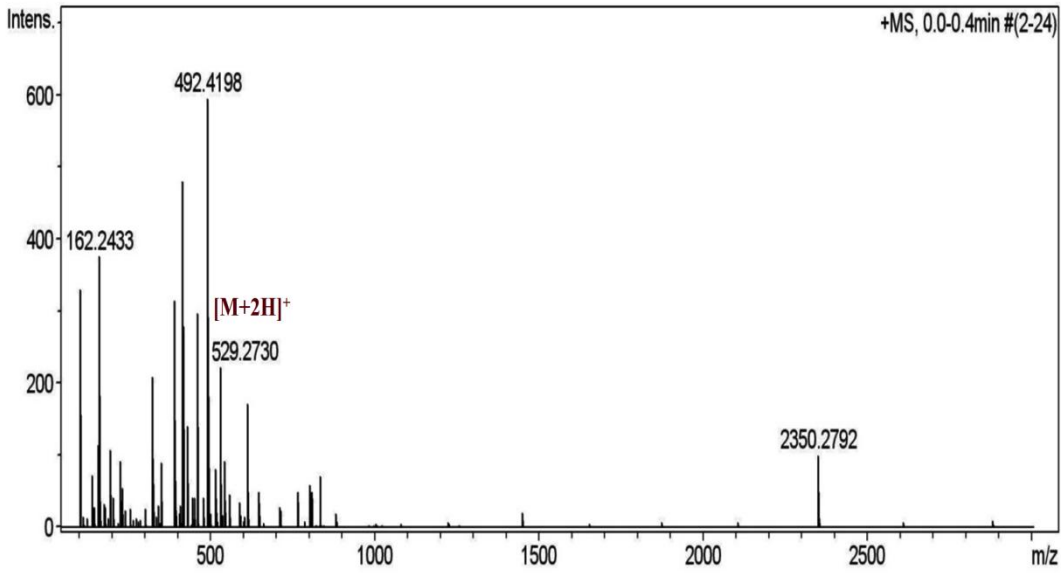

Figure S10. ESI MS spectrum of $Mn^{II}(1,1\text{-dithio})_2$ (1) complex.

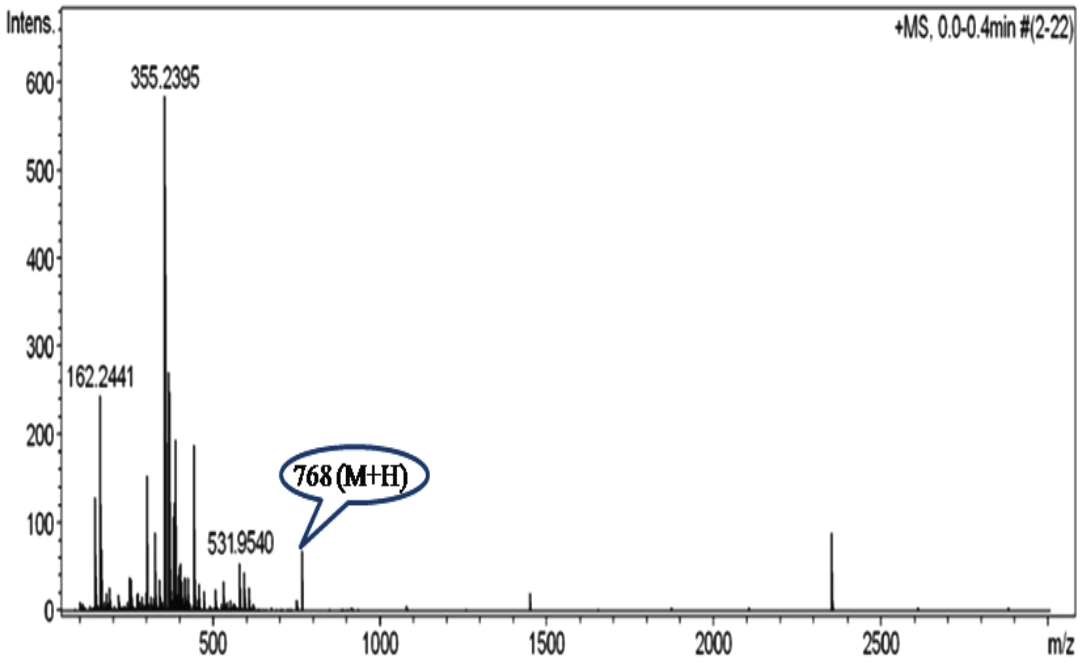

Figure S11. ESI MS spectrum of $Co^{III}(1,1\text{-dithio})_2$ (2) complex.

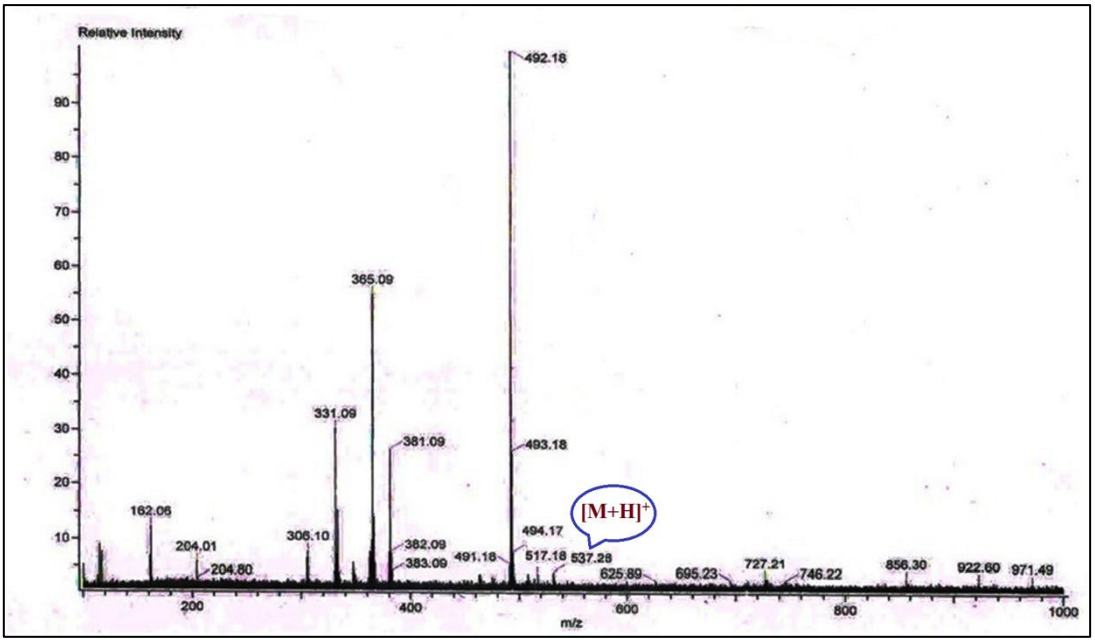

Figure S12. ESI MS spectrum of $Zn^{II}(1,1\text{-dithio})_2$ (3) complex.

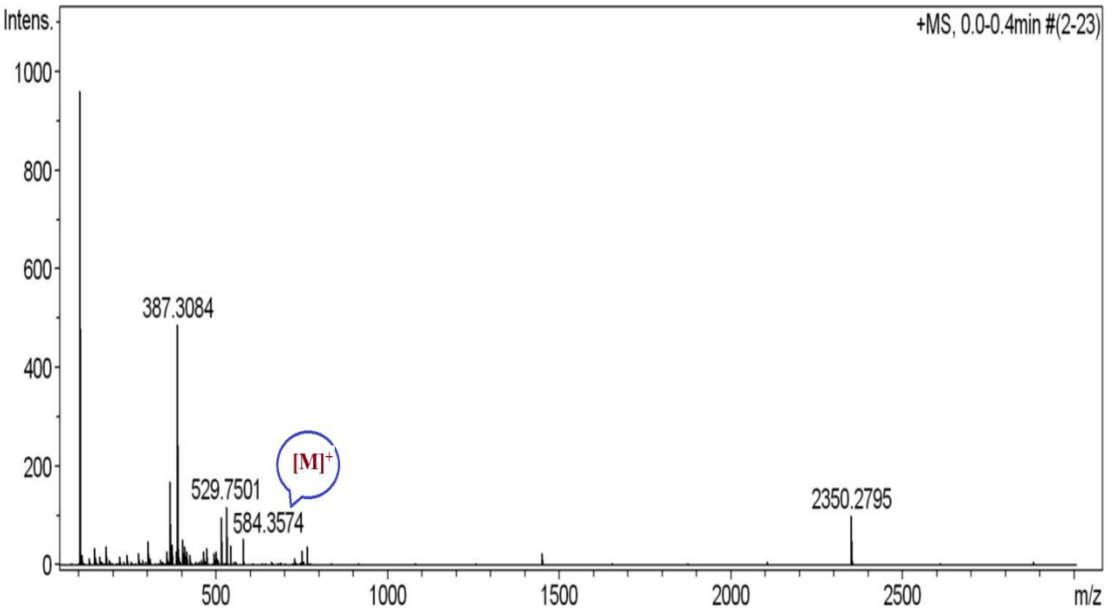

Figure S13. ESI MS spectrum of $Cd^{II}(1,1\text{-dithio})_2$ (4) complex.

3A.6.4. Fluorescence spectra

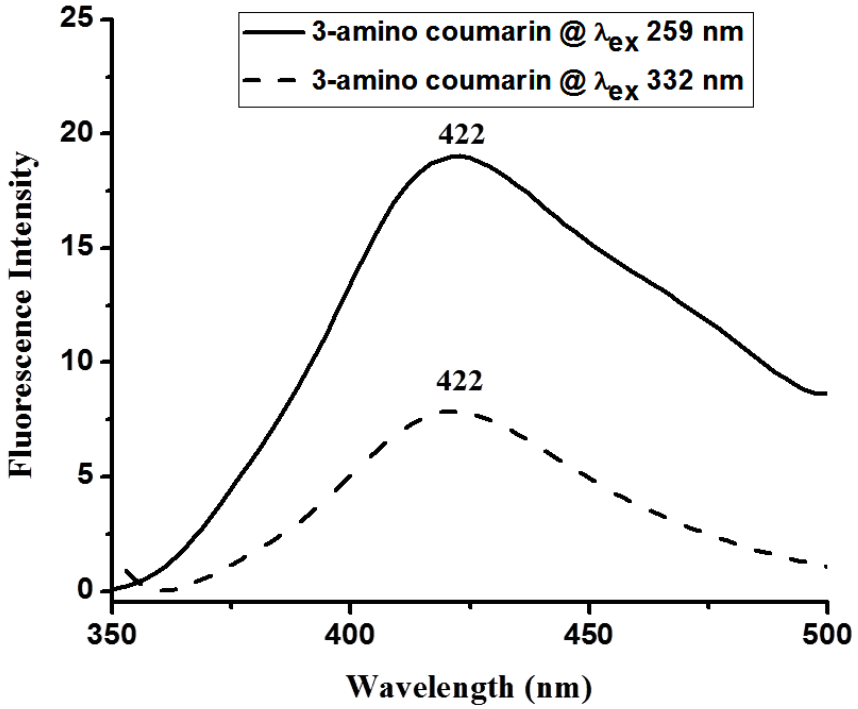

Figure S14. Fluorescence emission band of 3-aminocoumarin appreared at λ_{ex} 259 and 332 nm.

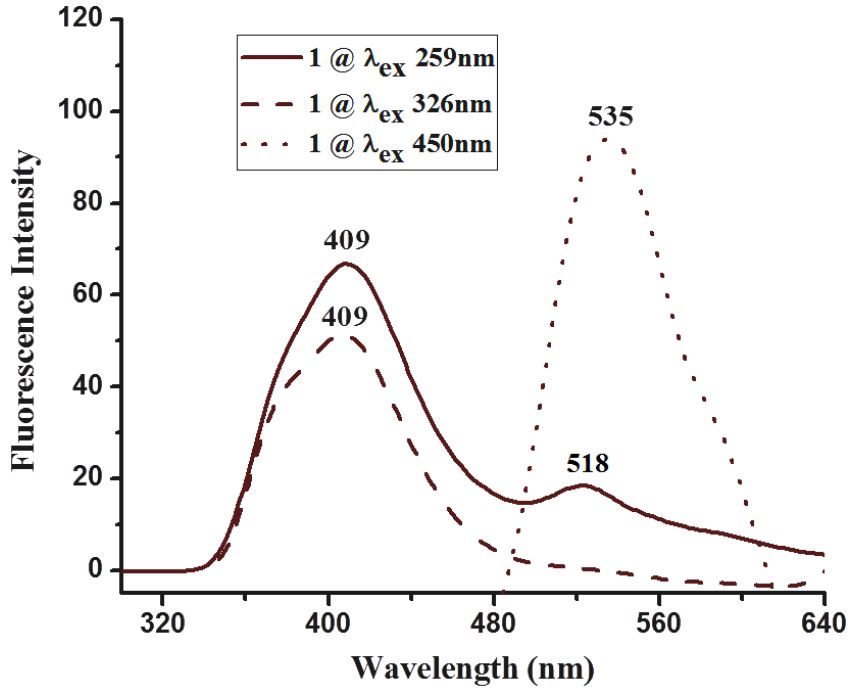

Figure S15. Fluorescence emission bands of complex **1** appreared at λ_{ex} 259, 326 and 450 nm.

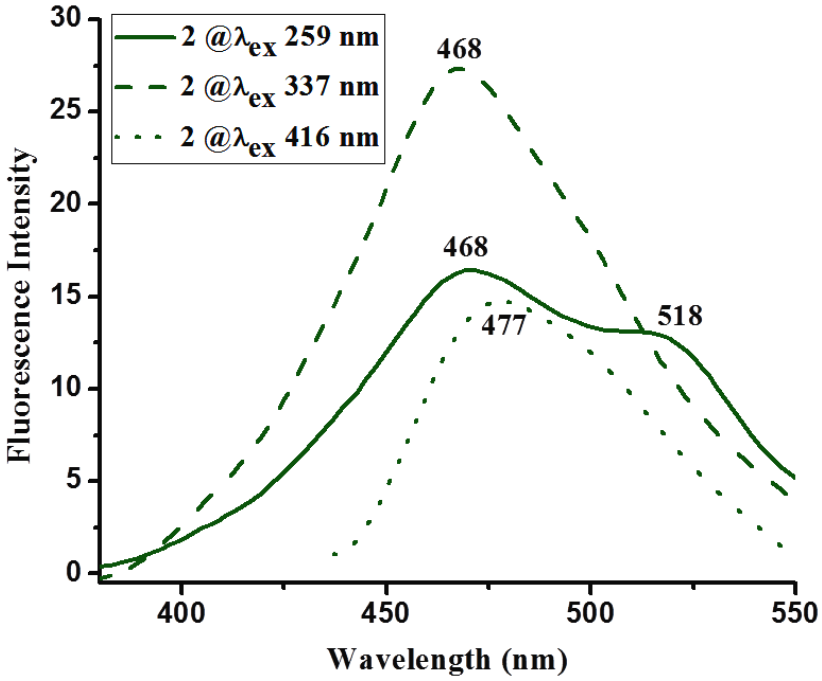

Figure S16. Fluorescence emission bands of complex **2** appreared at λ_{ex} 259, 337 and 416 nm.

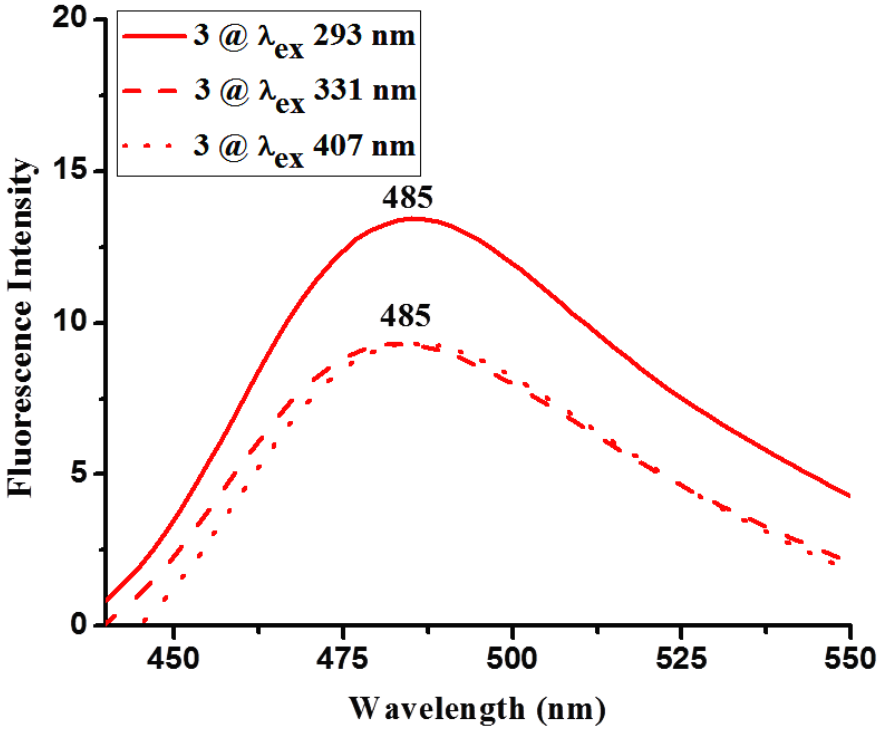

Figure S17. Fluorescence emission bands of complex **3** appreared at λ_{ex} 293, 331 and 407 nm.

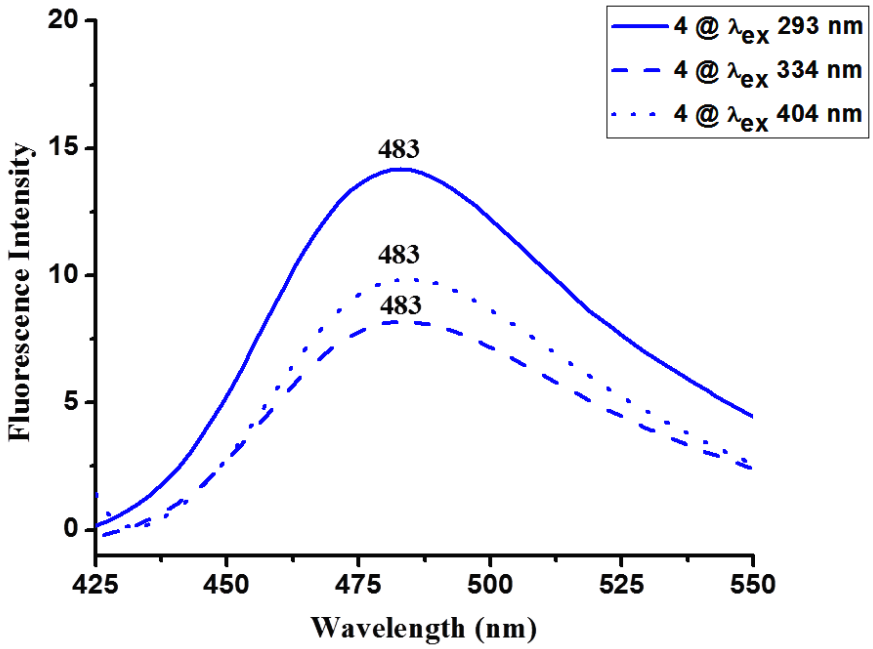

Figure S18. Fluorescence emission bands of complex **4** appreared at λ_{ex} 293, 334 and 404 nm.

3A.6.5. Geometrical optimization of complex 1:

Total energy: -1.8050 × 10^6 kcal/mol.

Cartesian Coordinates of Geometry of **1** optimized at the B3LYP/6-31G(d, p)/ lanL2DZ level.

Centre number	Atomic number	Atom type	Coordinates (Angstroms)		
			X	Y	Z
1	6	C	-9.14237	2.3772	-1.10987
2	6	C	-8.05407	2.78671	-1.89618
3	6	C	-6.79835	2.23345	-1.68877
4	6	C	-6.60074	1.25772	-0.69071
5	6	C	-7.71032	0.86792	0.07952
6	6	C	-8.97633	1.41528	-0.1175
7	6	C	-5.32546	0.64757	-0.42509
8	6	C	-5.21394	-0.28777	0.55723
9	6	C	-6.39365	-0.68756	1.35429
10	8	O	-7.58059	-0.07906	1.0655
11	8	O	-6.3514	-1.51932	2.23848
12	7	N	-4.08585	-1.00087	0.98155
13	6	C	-2.78751	-0.99772	0.61153
14	16	S	-1.7479	-2.09651	1.47049
15	16	S	-2.15423	0.02033	-0.63233
16	6	C	9.14198	2.3785	1.10857
17	6	C	8.05334	2.78923	1.89377
18	6	C	6.79765	2.23586	1.68647

19	6	C	6.60042	1.25882	0.68962
20	6	C	7.71033	0.86782	-0.07952
21	6	C	8.97632	1.41527	0.11741
22	6	C	5.32519	0.64847	0.42419
23	6	C	5.21404	-0.28823	-0.55688
24	6	C	6.39408	-0.68919	-1.35287
25	8	O	7.58096	-0.08045	-1.0643
26	8	O	6.35215	-1.52208	-2.23601
27	7	N	4.08607	-1.00176	-0.98077
28	6	C	2.78764	-0.99824	-0.61109
29	16	S	2.15399	0.02123	0.63142
30	16	S	1.74828	-2.09806	-1.46903
31	25	Mn	-9E-6	-1.11472	-4.7E-5
32	1	H	-10.12404	2.81151	-1.27389
33	1	H	-8.19481	3.53741	-2.66773
34	1	H	-5.95003	2.54442	-2.29231
35	1	H	-9.80058	1.08098	0.50355
36	1	H	-4.46753	0.94421	-1.01379
37	1	H	-4.33004	-1.64447	1.73675
38	1	H	10.12363	2.8129	1.2725
39	1	H	8.19379	3.54095	2.66439
40	1	H	5.94907	2.54775	2.28916
41	1	H	9.80084	1.08002	-0.50277
42	1	H	4.46702	0.94603	1.01206
43	1	H	4.3305	-1.64629	-1.7351